Modeling the Vibration of Spatial Flexible Mechanisms through an Equivalent Rigid Link System/Component Mode Synthesis Approach

Renato Vidoni[a], Paolo Gallina[b], Paolo Boscariol[c], Alessandro Gasparetto[c], Marco Giovagnoni[c]

[a]*FaST, Faculty of Science and Technology - Free University of Bozen-Bolzano, Piazza Università, 5 - Bolzano, Italy*
[b]*Dipartimento di Ingegneria Meccanica e Navale - University of Trieste (I)*
[c]*DIEGM, Department of Electrical, Management and Mechanical Eng. - University of Udine, Via delle Scienze, 208 - 33100 Udine, Italy*

Abstract

In this paper, a novel formulation for modeling the vibration of spatial flexible mechanism and robots is introduced. The formulation is based on the concepts of Equivalent Rigid Link System (ERLS) that allows to write the kinematic equations of motion of the Equivalent Rigid Link System as decoupled from the compatibility equations of the displacement at the joint. With respect to the available literature, in which the ERLS concept has been proposed together with a FEM approach (ERLS-FEM), the formulation is here extended through a modal approach and, in particular, a Component Mode Synthesis (CMS) technique, allowing to maintain a reduced-order system of dynamic equations even when a fine discretization is needed. The model has been validated numerically by comparison with the results obtained with the Adams-Flex™software, that implements the well known Floating Frame of Reference (FFR) approach, for a benchmark L-shaped mechanism, showing a good agreement between the two models.

Keywords: Equivalent Rigid Link System , Component mode Synthesis , Flexible-Link , Vibration , Deformation

1. Introduction

In industrial robotics, the demand for high performances and high operating has highlighted the need to study and develop lightweight manipulators. On the other hand, due to the dynamic effects of structural flexibility that arise in lightweight systems, the design and control are more difficult and accurate dynamic models are crucial for reaching an effective result.

In the last twenty years, many researchers focused their works on this topic, developing and refining dynamic models and formulations of the equations of motion for multibody rigid-flexible-link systems. First of all, single flexible-link mechanisms, then planar and finally spatial flexible-mechanisms were addressed. This research area, especially the 3D systems and their control, is still an open field of investigation (Shabana 1997, Benosman et al. 2002, Wasfy and Noor 2003, Dwivedy and Eberhard 2006, Tokhi and Azad 2008, Bauchau 2011, Garca-Vallejo et al. 2008, Ouyang et al. 2013, Choi and Cheon 2004).

In multibody dynamics, the classical approach is based on the rigid body dynamical model of the mechanism, then the elastic deformations are introduced to take the flexibility into account.

The elastic deformations of the bodies are influenced by the rigid gross motion and viceversa. The resultant complete dynamic formulation is a highly nonlinear and coupled set of partial differential equations.

In order to obtain a set of ordinary differential equations from these partial differential equations, thus a finite-dimensional problem, two methodologies have been adopted in the literature, namely the "nodal" approach, i.e. the Finite Element Method (FEM), and the "modal" approach, i.e. the Assumed Mode Method (AMM) (Dwivedy and Eberhard 2006, Dietz et al. 2003, Ge et al. 1997, Wang et al. 1996, Martins et al. 2003, Naganathan and Soni 1988, Nagarajan and Turcic 1990, Theodore and Ghosal 1995, Kalra and Sharan 1991).

Especially in case of large rotations and small vibration displacements, the most adopted and well-known formulation, that includes both the effect of the rigid body motion on the elastic deformation and the effect of the elasticity on the rigid body motion, is the so-called Floating Frame of Reference (FFR) formulation (Shabana 1997, 2005). In the FFR formulation, a system of coupled differential equations is obtained with no separation between the rigid body motion and the elastic deformation of the flexible body.

By approaching the problem from a robotic point of view, the main drawback of the FFR is related to the constraint conditions since the connection through mechanical joints between different deformable bodies is expressed by coupled constraint equations that do not have an immediate formulation.

In this work, a novel approach for dynamic modelling of spatial flexible mechanisms under the condition of large displacements and small deformations is presented.

The method is based on an Equivalent Rigid Link System (ERLS), firstly introduced in (Turcic and Midha 1984b,a, Turcic et al. 1984, Chang and Hamilton 1991), that enables to decouple the kinematic equations of the Equivalent Rigid Link System from the compatibility equations of the displacements at the joints. Thanks to the ERLS, the standard concepts of 3-D kinematics can be adopted to formulate and solve the system kinematics. In previous works, the ERLS concept has been exploited together with a FEM approach (ERLS-FEM), to model firstly planar flexible-link mechanisms (Giovagnoni 1994, Gasparetto 2001, Gasparetto and Zanotto 2006, Caracciolo et al. 2005) and then 3D systems (Vidoni et al. 2014, 2013, Gasparetto et al. 2013). The approach has been also exploited and applied for control purposes (Trevisani 2003, Caracciolo et al. 2005, Boscariol and Zanotto 2012, Boschetti et al. 2012).

One of the limitations of the ERLS-FEM model is that the number of Degrees of Freedom (DoFs) of the system, which is directly related to the mesh refinement, should be maintained low if a low computational time and a real-time model-based control is required.

In this work, the ERLS approach, that can be applied to mechanisms with rotational DoFs or prismatic joints in which one of the links is the ground link, is extended through a modal approach, in order to obtain a more flexible solution based upon a reduced-order system of equations. The compatibility with both rotational and prismatic joints is inherited by the use of Denavit-Hartemberg (Denavit and Hartenberg 1955) procedure for the definition and the solution of the kinematics of the mechanism.

To the best of our knowledge, this is the first work in which the ERLS concept is applied in order to formulate the dynamics of spatial flexible mechanisms with a Component Mode Synthesis (CMS) technique.

In this paper, after the description of the kinematics of the ERLS and of the flexible-link mechanism (Section 2), the main differences between the ERLS and the FFR formulations are highlighted (Section 3). Section 4 deals with the derivation of the virtual work term contributions while Section 5 collects the different terms into the equations of motion. The numerical

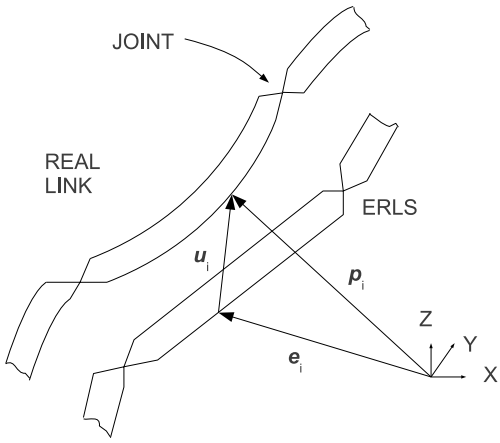

Figure 1: Model of the mechanism and kinematic definitions

implementation of the model and its validation is given in Section 6 through a comparison with the Adams-Flex™multibody dynamic software for a benchmark flexible mechanism.

2. CMS and ERLS kinematics

Let us consider Fig. 1, which shows the kinematic definitions: $\boldsymbol{u}_i$ represents the nodal displacement vector of the ith link, $\boldsymbol{e}_i$ is the nodal position vector for the ith element of the ERLS and $\boldsymbol{p}_i$ is the absolute nodal position vector. The index i spans from 1 to l, where l is the number of links of the mechanism.

Given the definition of the vectors above, the following holds:

$$\boldsymbol{p}_i = \boldsymbol{e}_i + \boldsymbol{u}_i \tag{1}$$

Let us express the nodal displacements $\boldsymbol{u}_i$ of the i-th link as functions of a given number of eigenvectors $\boldsymbol{U}_i$ and modal coordinates $\boldsymbol{q}_i$, namely

$$\boldsymbol{u}_i = \boldsymbol{U}_i \boldsymbol{q}_i \tag{2}$$

Eigenvectors and eigenvalues can be calculated according to the chosen modal reduction approach, e.g. the Guyan reduction (Qu 2004). With respect to the previous ERLS-FEM formulations, that usually deal with flexible beam type links, the model extension through a modal approach will allow to work with whatsoever flexible- or rigid- link shape and finite elements.

Assumption 1′. *The CMS theory requires to choose the modal coordinates in such a way that they comprehend all the modal coordinates related to the rigid-motion of the link, plus at least one modal coordinate related to the main vibration mode of the link.*

If a link is assumed to be rigid, only eigenvectors related to the rigid-motion are considered (6 eigenvectors for the 3D case, 3 eigenvectors for the 2D case).

Let $\hat{\boldsymbol{u}}_i = \boldsymbol{S}_i \boldsymbol{u}_i$ be the displacements of the joint belonging to the link i and $\hat{\boldsymbol{u}}_{i+1} = \boldsymbol{S}_{i+1} \boldsymbol{u}_{i+1}$ the displacements of the joint belonging to the link $i+1$, where matrices $\boldsymbol{S}_i$ and $\boldsymbol{S}_{i+1}$ are introduced

Table 1: Main Nomenclature

symbol	explanation
$\boldsymbol{u}_i$	nodal displacement vector of the i-th link
$\boldsymbol{e}_i$	nodal position vector of the i-th link
$\boldsymbol{p}_i$	absolute nodal position vector for the i-th link
$\boldsymbol{U}_i$	eigenvectors of the i-th link
$\boldsymbol{q}_i$	modal coordinates of the i-th link
$\boldsymbol{S}_i$	matrix for the selection of the joint displacements among the nodal displacements
$\boldsymbol{T}_{i,j}$	local-to-local transformation matrix between the local reference frames of i-th and j-th link
$\boldsymbol{\theta}$	vector of joint positions
$\boldsymbol{C}$	matrix of compatibility relationships
$\boldsymbol{q}_r$	vector of rigid-motion modal coordinates
$\boldsymbol{q}_d$	vector of elastic modal coordinates
$\boldsymbol{C}_r, \boldsymbol{C}_r$	partitions of $\boldsymbol{C}$
$\boldsymbol{D}$	matrix of relationships between vibrational modal coordinates and rigid-body modal coordinates
$\boldsymbol{E}$	vector containing the partial derivatives matrices of $\boldsymbol{C}$ with respect to the rigid DoFs as defined in eq. (13)
$\boldsymbol{G}$	$\stackrel{\text{def}}{=} -\boldsymbol{C}_r^{+}(\boldsymbol{\theta})\boldsymbol{E}(\boldsymbol{\theta}, \boldsymbol{q})$
$\overline{\boldsymbol{R}}$	local-to-global rotation matrix for the whole mechanism
$\boldsymbol{G}_X$	velocity of point X
$\boldsymbol{a}_X$	acceleration of point X
$\hat{\boldsymbol{B}}$	matrix of relationships between the linear velocities of three non aligned nodes with respect to the velocity of the first one (see appendix A)
$\boldsymbol{U}_r, \boldsymbol{U}_d$	rigid-body and elastic mode eigenvectors, respectively
$\overline{\boldsymbol{\Omega}}$	matrix of angular speeds for the whole mechanism
$\boldsymbol{\phi}$	vector of virtual rotational displacements
$\boldsymbol{M}$	mass matrix
$\boldsymbol{\Phi}$	matrix of absolute rotational displacement
$\boldsymbol{\Omega}$	skew symmetric matrix of absolute angular velocities
$\boldsymbol{A}$	skew symmetric matrix of absolute angular accelerations
$\delta\boldsymbol{\Phi}$	skew symmetric matrix of virtual rotational displacements represented in the local reference frame
$\boldsymbol{H}$	elastic energy of each link
$\boldsymbol{K}$	stiffness matrix of each link
$\boldsymbol{\Gamma}$	diagonal matrix of the squares of natural frequencies of each link
$\boldsymbol{f}_g$	vector of gravity forces
$\boldsymbol{g}_l$	vector of gravity acceleration components expressed in the local reference frame
$\hat{\boldsymbol{I}}$	matrix of $\hat{\boldsymbol{i}}_i$ components (see Appendix D)
$\boldsymbol{f}$	vector of generalized forces acting on each link
δW	virtual work
$\hat{\boldsymbol{U}}_f$	submatrix of $\boldsymbol{U}$
$\boldsymbol{J}(\boldsymbol{\theta})$	Jacobian matrix of the ERLS
$\boldsymbol{V}_i^{\mathrm{o}}$	block diagonal selection matrix used in eq. (69)
$\boldsymbol{N}$	matrix that relates the vector of the independent DoFs with the overall system DoFs the used in eq. (69)
$\boldsymbol{L}_i$	selection matrix for the elements independent form virtual displacements and accelerations
$\tilde{\boldsymbol{l}}_i$	submatrix of $\boldsymbol{l}$ elements independent from accelerations
$\boldsymbol{L}$	selection matrix for the elements independent form virtual displacements and accelerations for the whole mechanism
$\tilde{\boldsymbol{l}}$	submatrix of $\boldsymbol{l}$ elements independent from accelerations for the whole mechanism
$\boldsymbol{\omega}$	absolute angular velocity
$\boldsymbol{\alpha}$	absolute angular acceleration

just to extract the proper joint displacements from all the nodal displacements $\boldsymbol{u}_i$, hence they are made of ”0” and ”1” only.

In terms of modal coordinates, the joint displacements are given by: $\hat{\boldsymbol{u}}_i = \boldsymbol{S}_i\boldsymbol{U}_i\boldsymbol{q}_i$ and $\hat{\boldsymbol{u}}_{i+1} = \boldsymbol{S}_{i+1}\boldsymbol{U}_{i+1}\boldsymbol{q}_{i+1}$

The following equation accounts for the compatibility condition at the i-th joint:

$$\hat{\boldsymbol{u}}_{i+1} = \boldsymbol{T}_{i+1,i}\hat{\boldsymbol{u}}_i \tag{3}$$

where $\boldsymbol{T}_{i+1,i}(\boldsymbol{\theta})$ is local-to-local transformation matrix between the two reference frames of the ELRLs associated to the two consecutive links i and $i+1$. Transformation matrices are function of the joint parameters vector $\boldsymbol{\theta} = \left\{\theta_1 \quad \theta_2 \quad \cdots \quad \theta_n\right\}^T$.

Eq. 3 can be rewritten as:

$$\boldsymbol{S}_{i+1}\boldsymbol{U}_{i+1}\boldsymbol{q}_{i+1} = \boldsymbol{T}_{i+1,i}(\boldsymbol{\theta})\boldsymbol{S}_i\boldsymbol{U}_i\boldsymbol{q}_i \tag{4}$$

or

$$\left[\begin{array}{c|c} -\boldsymbol{T}_{i+1,i}(\boldsymbol{\theta})\boldsymbol{S}_i\boldsymbol{U}_i & \boldsymbol{S}_{i+1}\boldsymbol{U}_{i+1} \end{array}\right]\left[\begin{array}{c}\boldsymbol{q}_i\\ \hline \boldsymbol{q}_{i+1}\end{array}\right] = \boldsymbol{0} \tag{5}$$

Since the equations in (4) (one for each joint) are linear with respect to the modal coordinates, the following comprehensive compatibility equation can be assembled:

$$\boldsymbol{C}(\boldsymbol{\theta})\boldsymbol{q} = \boldsymbol{0} \tag{6}$$

where:

$$\boldsymbol{C}(\boldsymbol{\theta}) = \begin{bmatrix} \boldsymbol{S}_1\boldsymbol{U}_1 & \boldsymbol{0} & \cdots & \cdots & \cdots & \boldsymbol{0} \\ -\boldsymbol{T}_{1,2}(\boldsymbol{\theta})\boldsymbol{S}_1\boldsymbol{U}_1 & \boldsymbol{S}_2\boldsymbol{U}_2 & \boldsymbol{0} & \cdots & \cdots & \boldsymbol{0} \\ \boldsymbol{0} & -\boldsymbol{T}_{2,3}(\boldsymbol{\theta})\boldsymbol{S}_2\boldsymbol{U}_2 & \boldsymbol{S}_3\boldsymbol{U}_3 & \boldsymbol{0} & \cdots & \boldsymbol{0} \\ \boldsymbol{0} & \boldsymbol{0} & \cdots & \ddots & \ddots & \boldsymbol{0} \\ \boldsymbol{0} & \boldsymbol{0} & \boldsymbol{0} & \ddots & \ddots & \boldsymbol{0} \\ \boldsymbol{0} & \cdots & & & -\boldsymbol{T}_{n-1,n}(\boldsymbol{\theta})\boldsymbol{S}_{n-1}\boldsymbol{U}_{n-1} & \boldsymbol{S}_n\boldsymbol{U}_n \\ \boldsymbol{0} & \boldsymbol{0} & \cdots & \cdots & \boldsymbol{0} & -\boldsymbol{T}_{n,n+1}(\boldsymbol{\theta})\boldsymbol{S}_n\boldsymbol{U}_n \end{bmatrix} \tag{7}$$

and

$$\boldsymbol{q} = \left[\boldsymbol{q_1}^T \quad \boldsymbol{q_2}^T \quad \cdots \quad \boldsymbol{q_n}^T\right]^T \tag{8}$$

Note that the coefficient matrix $\boldsymbol{C}$ depends only on the joint parameters and that $\boldsymbol{q}$ contains both the rigid-body and the elastic modal coordinates.

As far as the ERLS mechanism is considered, the total number of DoFs of all the links without constraints m is related to the total number of DoFs of the ERLS mechanism n through the relationship

$$m - \nu = n \tag{9}$$

The numbers of rows of $\boldsymbol{C}$ equals the number of constraints ν imposed by the joints. The number of columns equals the total number of modal coordinates and is given by the sum of the number of the rigid-body modal coordinates m and the number of the elastic modal coordinates d. For eq. 6, the dimensions of $\boldsymbol{C}$ are $\nu \times (m + d) = (m - n) \times (m + d)$. Therefore, the linear system (6) is underdetermined and the solution is of the form ∞^{n+d}.

All the rigid-motion modal coordinates and the elastic modal coordinates can be gathered respectively into two separate vectors $\boldsymbol{q_r}$ and $\boldsymbol{q_d}$. Thus, the system (6) can be rearranged as follows:

$$\boldsymbol{C}_r\boldsymbol{q}_r + \boldsymbol{C}_d\boldsymbol{q}_d = \boldsymbol{0} \tag{10}$$

wherein the submatrix $\boldsymbol{C}_r$ has dimensions $v \times m$ and $\boldsymbol{C}_d$ has dimensions $v \times d$. Note that, because of eq. 9, $v < m$, i.e. the number of unknowns is greater than the number of equations.

By using the right pseudo-inverse $\boldsymbol{C}_r^+ = \boldsymbol{C}_r^T(\boldsymbol{C}_r\boldsymbol{C}_r^T)^{-1}$ (Ben-Israel and Greville 2003), the system (10) can be solved with respect to $\boldsymbol{q}_r$, namely $\boldsymbol{q}_r = -\boldsymbol{C}_r^+\boldsymbol{C}_d\boldsymbol{q}_d$. In this way, the minimum norm solution is chosen for the unknown $\boldsymbol{q}_r$ vector. Eventually, introducing a new matrix $\boldsymbol{D}(\boldsymbol{\theta}) \stackrel{\text{def}}{=} -\boldsymbol{C}_r^+(\boldsymbol{\theta})\boldsymbol{C}_d(\boldsymbol{\theta})$ it is possible to represent the vibration modal coordinates as functions of rigid-body modal coordinates and joint parameters (ERLS coordinates):

$$\boldsymbol{q}_r = \boldsymbol{D}(\boldsymbol{\theta})\boldsymbol{q}_d \tag{11}$$

It should be remarked that, according to (11), the rigid-body modal coordinates are function of $\boldsymbol{\theta}$ and $\boldsymbol{q}_d$ only. Note that, if $\boldsymbol{q}_d = \boldsymbol{0}$ then $\boldsymbol{q}_r = \boldsymbol{0}$. In other words, if all the links are assumed rigid, the remaining DoFs are the ones of the ERLS.

According to the literature, the selection of the interior modes to be retained to keep model dimensions to a minimum while preserving system response accuracy is still an open field of investigation; indeed, the choice of the reduction strategy and dimension of the reduced-order model is generally left to the experience. Often, only the lower frequency modes are retained. In Koutsovasilis and Beitelschmidt 2008 and Besselink et al. 2013 a comparison of model reduction techniques have been made. Recently, a new approach based on an energy-based coefficient has been proposed for resonant systems by Palomba et al. 2014. In this work, in order to be able to compare the results with the FFR Adams™ implementation (see Section 6), a classical Craig-Bampton approach (Craig and Bampton 1968), where the lower frequency modes are retained, has been adopted.

2.1. Derivative terms

In order to implement the dynamic analysis of the complete mechanism, it is necessary to derive all the velocity and acceleration terms as functions of $\boldsymbol{\theta}$, $\boldsymbol{q}_d$ and their derivatives.

By differentiating eq. 6 with respect to time, it yields: $\dot{\boldsymbol{C}}\boldsymbol{q} + \boldsymbol{C}\dot{\boldsymbol{q}} = \boldsymbol{0}$ which can be written as:

$$\sum_k \frac{\partial \boldsymbol{C}}{\partial \theta_k}\boldsymbol{q}\dot{\theta}_k + \boldsymbol{C}\dot{\boldsymbol{q}} = \boldsymbol{0} \tag{12}$$

Let us define:

$$\boldsymbol{E}(\boldsymbol{\theta}, \boldsymbol{q}) \stackrel{\text{def}}{=} [\frac{\partial \boldsymbol{C}}{\partial \theta_1}\boldsymbol{q} \ldots \frac{\partial \boldsymbol{C}}{\partial \theta_n}\boldsymbol{q}] \tag{13}$$

By replacing (13) into (12), one obtains: $\boldsymbol{E}\dot{\boldsymbol{\theta}} + \boldsymbol{C}\dot{\boldsymbol{q}} = \boldsymbol{0}$ and, after splitting the coefficient matrix $\boldsymbol{C}$ according to (10), (12) becomes $\boldsymbol{E}\dot{\boldsymbol{\theta}} + \boldsymbol{C}_d\dot{\boldsymbol{q}}_d + \boldsymbol{C}_r\dot{\boldsymbol{q}}_r = \boldsymbol{0}$.

The previous equation can be solved with respect to the rigid-motion modal coordinate derivative terms by exploiting the pseudo-inverse, namely:

$\dot{\boldsymbol{q}}_r = -\boldsymbol{C}_r^+\boldsymbol{C}_d\dot{\boldsymbol{q}}_d - \boldsymbol{C}_r^+\boldsymbol{E}\dot{\boldsymbol{\theta}}$. The final equation is obtained by introducing the matrix $\boldsymbol{G}(\boldsymbol{\theta},\boldsymbol{q}) \stackrel{\text{def}}{=} -\boldsymbol{C}_r^+(\boldsymbol{\theta})\boldsymbol{E}(\boldsymbol{\theta},\boldsymbol{q})$

$$\dot{\boldsymbol{q}}_r = \boldsymbol{D}(\boldsymbol{\theta})\dot{\boldsymbol{q}}_d + \boldsymbol{G}(\boldsymbol{\theta},\boldsymbol{q})\dot{\boldsymbol{\theta}} \tag{14}$$

which expresses the relationship between the velocities of the rigid-body modal coordinates and the velocities of the independent variables. The equation can be represented in terms of virtual displacements:

$$\delta\boldsymbol{q}_r = \boldsymbol{D}(\boldsymbol{\theta})\delta\boldsymbol{q}_d + \boldsymbol{G}(\boldsymbol{\theta},\boldsymbol{q})\delta\boldsymbol{\theta} \tag{15}$$

2.2. Acceleration terms

By differentiating twice eq. 6 with respect to time, one obtains:

$$\ddot{\boldsymbol{C}}\boldsymbol{q} + 2\dot{\boldsymbol{C}}\dot{\boldsymbol{q}} + \boldsymbol{C}\ddot{\boldsymbol{q}} = \boldsymbol{0} \tag{16}$$

The second derivative of the coefficient matrix is :

$$\ddot{\boldsymbol{C}} = \frac{d}{dt}\sum_k \frac{\partial \boldsymbol{C}}{\partial\theta_k}\dot{\theta}_k = \sum_j\sum_k \frac{\partial^2\boldsymbol{C}}{\partial\theta_j\partial\theta_k}\dot{\theta}_j\dot{\theta}_k + \sum_k \frac{\partial\boldsymbol{C}}{\partial\theta_k}\ddot{\theta}_k \tag{17}$$

Let us introduce the notations:

$$\boldsymbol{h}(\boldsymbol{\theta},\dot{\boldsymbol{\theta}},\boldsymbol{q}) \stackrel{\text{def}}{=} \left(\sum_j\sum_k \frac{\partial^2\boldsymbol{C}}{\partial\theta_j\partial\theta_k}\dot{\theta}_j\dot{\theta}_k\right)\boldsymbol{q} \tag{18}$$

and

$$\boldsymbol{c}(\boldsymbol{\theta},\dot{\boldsymbol{\theta}},\dot{\boldsymbol{q}}) \stackrel{\text{def}}{=} \dot{\boldsymbol{C}}\dot{\boldsymbol{q}} = \left(\sum_k \frac{\partial\boldsymbol{C}}{\partial\theta_k}\dot{\theta}_k\right)\dot{\boldsymbol{q}} \tag{19}$$

Multiplying both sides of eq. 17 by $\boldsymbol{q}$ and using (13) and (18), it yields:

$$\ddot{\boldsymbol{C}}\boldsymbol{q} = \boldsymbol{h}(\boldsymbol{\theta},\dot{\boldsymbol{\theta}},\boldsymbol{q}) + \boldsymbol{E}(\boldsymbol{\theta},\boldsymbol{q})\ddot{\boldsymbol{\theta}} \tag{20}$$

Replacing eq.s 16 and 19 into 20, the second derivative of eq. 6 can be written as:

$$\boldsymbol{h}(\boldsymbol{\theta},\dot{\boldsymbol{\theta}},\boldsymbol{q}) + \boldsymbol{E}(\boldsymbol{\theta},\boldsymbol{q})\ddot{\boldsymbol{\theta}} + 2\boldsymbol{c}(\boldsymbol{\theta},\dot{\boldsymbol{\theta}},\dot{\boldsymbol{q}}) + \boldsymbol{C}(\boldsymbol{\theta})\ddot{\boldsymbol{q}} = \boldsymbol{0} \tag{21}$$

By splitting matrix $\boldsymbol{C}$ according to eq. 10 and solving the resulting system with respect to $\ddot{\boldsymbol{q}}_r$, the acceleration of rigid-body modal coordinates as functions of the independent coordinates is computed:

$$\ddot{\boldsymbol{q}}_r = -\boldsymbol{C}_r^+(\boldsymbol{\theta})\boldsymbol{h}(\boldsymbol{\theta},\dot{\boldsymbol{\theta}},\boldsymbol{q}) - \boldsymbol{C}_r^+(\boldsymbol{\theta})\boldsymbol{E}(\boldsymbol{\theta},\boldsymbol{q})\ddot{\boldsymbol{\theta}} - 2\boldsymbol{C}_r^+(\boldsymbol{\theta})\boldsymbol{c}(\boldsymbol{\theta},\dot{\boldsymbol{\theta}},\dot{\boldsymbol{q}}) - \boldsymbol{C}_r^+(\boldsymbol{\theta})\boldsymbol{C}_d(\boldsymbol{\theta})\ddot{\boldsymbol{q}}_d \tag{22}$$

By adopting the notation:

$$\boldsymbol{n}(\boldsymbol{\theta},\dot{\boldsymbol{\theta}},\boldsymbol{q},\dot{\boldsymbol{q}}) \stackrel{\text{def}}{=} -\boldsymbol{C}_r^+(\boldsymbol{\theta})\boldsymbol{h}(\boldsymbol{\theta},\dot{\boldsymbol{\theta}},\boldsymbol{q}) - 2\boldsymbol{C}_r^+(\boldsymbol{\theta})\boldsymbol{c}(\boldsymbol{\theta},\dot{\boldsymbol{\theta}},\dot{\boldsymbol{q}}) \tag{23}$$

eq. 22 can be rewritten as:

$$\ddot{\boldsymbol{q}}_r = \boldsymbol{G}(\boldsymbol{\theta},\boldsymbol{q})\ddot{\boldsymbol{\theta}} + \boldsymbol{D}(\boldsymbol{\theta})\ddot{\boldsymbol{q}}_d + \boldsymbol{n}(\boldsymbol{\theta},\dot{\boldsymbol{\theta}},\boldsymbol{q},\dot{\boldsymbol{q}}) \tag{24}$$

3. Differences between the ERLS and the FFR formulations

It is now possible to enumerate the differences between the ERLS and FFR formulations.

1. In the FFR approach the ith deformed body does not present rigid displacements with respect to the ith link, in the sense that there are not rigid motions of the deformed body with respect to the local reference frame. On the other hand, rigid displacements are required for the ERLS approach: they are defined by the values of the rigid-body modal coordinates.
2. In the FFR case, joint parameters and deformation modal values are coupled in the *kinematic equations*. Indeed, the constraint equations depend both on the elastic deformations and on the reference motion of the elastic bodies. In the Equivalent Rigid Link System approach the *kinematic equations* contain just the joint parameters, since deformation modal values are present in the compatibility condition at the joints. This means that, as highlighted in previous works e.g. Vidoni et al. 2013, the *kinematic equations* of the ERLS are decoupled from the compatibility equations of the displacement at the joints.
3. As a consequence of 2, if a closed-form solution of the *kinematic equations* is available, it can be employed without resorting to iterative algorithm procedures.
4. Moreover, thanks to 2, for the ERLS approach the choice of independent variables is not problematic as it is, on the other hand, for the FFR approach, as stated in (Shabana 2005).
5. The ERLS approach allows to work directly with a classical Denavit-Hartenberg (Denavit and Hartenberg 1955) formulation as well as to cope with the flexible-link robot as if it were a rigid-link one.

4. Virtual work contributions

4.1. Virtual work of inertial forces for a single link

Let us drop, for sake of clarity, the i subscript which indicates the link to which each vector refers to. Let **p** be the vector containing the global coordinates of all the nodes of the link, **e** the vector containing the global coordinates of all the nodes belonging to the ERLS and **u** the vector containing all the nodal displacements. These vectors satisfy the equation

$$\boldsymbol{p} = \boldsymbol{e} + \boldsymbol{u} \tag{25}$$

according to notation of eq. 1. Note that all terms are represented with respect to the global reference frame. **u** can be expressed on terms of modal coordinates by the relationship

$$\boldsymbol{u} = \bar{\boldsymbol{R}}\boldsymbol{U}\boldsymbol{q} \tag{26}$$

where the matrix $\bar{\boldsymbol{R}}$ contains on the main diagonal the blocks of the local-to-global rotational matrices T_i. Thus, the nodal virtual displacements and the second derivative of nodal displacements are

$$\delta\boldsymbol{u} = \delta\bar{\boldsymbol{R}}\boldsymbol{U}\boldsymbol{q} + \bar{\boldsymbol{R}}\boldsymbol{U}\delta\boldsymbol{q} \tag{27}$$

$$\ddot{\boldsymbol{u}} = \ddot{\bar{\boldsymbol{R}}}\boldsymbol{U}\boldsymbol{q} + 2\dot{\bar{\boldsymbol{R}}}\boldsymbol{U}\dot{\boldsymbol{q}} + \bar{\boldsymbol{R}}\boldsymbol{U}\ddot{\boldsymbol{q}} \tag{28}$$

In order to compute the virtual displacements and the acceleration related to the ERLS, it is necessary to introduce the general formulation of velocity and acceleration of a generic point associated to the rigid-body, i.e. to the link of the ERLS.

For a point $\boldsymbol{P}$, the velocity and the acceleration measured with respect to a point $\boldsymbol{O}$ are:

$$\boldsymbol{v}_p = \boldsymbol{v}_o - (\boldsymbol{P} - \boldsymbol{O}) \wedge \boldsymbol{\omega} \tag{29}$$

$$\boldsymbol{a}_p = \boldsymbol{a}_o - (\boldsymbol{P} - \boldsymbol{O}) \wedge \boldsymbol{\alpha} + \boldsymbol{\omega} \wedge (\boldsymbol{v}_p - \boldsymbol{v}_o) \tag{30}$$

Let us choose three different non-aligned nodes, identified by the subscripts 0, 1 and 2. The velocities of the last two nodes with respect to the first one are: $\boldsymbol{v}_1 = \boldsymbol{v}_0 - (\boldsymbol{P}_1 - \boldsymbol{P}_0) \wedge \boldsymbol{\omega}$ and $\boldsymbol{v}_2 = \boldsymbol{v}_0 - (\boldsymbol{P}_2 - \boldsymbol{P}_0) \wedge \boldsymbol{\omega}$; using a matrix notation, the following holds:

$$\begin{bmatrix} \boldsymbol{v}_0 \\ \boldsymbol{v}_1 \\ \boldsymbol{v}_2 \end{bmatrix} = \hat{\boldsymbol{B}} \begin{bmatrix} \boldsymbol{v}_0 \\ \boldsymbol{\omega} \end{bmatrix} \tag{31}$$

where $\hat{\boldsymbol{B}}$ is a 9×6 matrix defined in Appendix A.

The matrix $\boldsymbol{U}$ can be split into two blocks: the columns of the first one are the rigid-body mode eigenvectors while the columns of the second one are the deformation mode eigenvectors: $\boldsymbol{U} = \begin{bmatrix} \boldsymbol{U}_r & | & \boldsymbol{U}_d \end{bmatrix}$.

Let us extract from the matrix $\boldsymbol{U}_r$ the submatrix $\hat{\boldsymbol{U}}_r$ whose rows contain just the components related to the nodes 0,1 and 2. Since $\boldsymbol{U}_r$ is made with rigid-body mode vectors, there exists an unknown vector $\boldsymbol{x}$ which satisfies:

$$\begin{bmatrix} \boldsymbol{v}_0 \\ \boldsymbol{v}_1 \\ \boldsymbol{v}_2 \end{bmatrix} = \hat{\boldsymbol{U}}_r \boldsymbol{x} \tag{32}$$

By equating eq.s 31 and 32, and using the left pseudo-inverse to obtain the solution that minimizes the norm of the error (Ben-Israel and Greville 2003), it yields:

$$\boldsymbol{x} = \tilde{\boldsymbol{B}} \begin{bmatrix} \boldsymbol{v}_0 \\ \boldsymbol{\omega} \end{bmatrix} \tag{33}$$

where: $\tilde{\boldsymbol{B}} = (\hat{\boldsymbol{U}}_r^T \hat{\boldsymbol{U}}_r)^{-1} \hat{\boldsymbol{U}}_r^T \hat{\boldsymbol{B}}$.

By means of the matrix $\boldsymbol{U_r}$ introduced in eq. 26, all the velocities of the nodes belonging to the ERLS (expressed with respect to the reference frame of the links) are obtained as a function of the velocity of node 0 and the angular velocity vector, in the form:

$$\dot{\boldsymbol{e}} = \bar{\boldsymbol{R}} \boldsymbol{U}_r \tilde{\boldsymbol{B}} \begin{bmatrix} \boldsymbol{v}_0 \\ \boldsymbol{\omega} \end{bmatrix} \tag{34}$$

Note that the matrix $\tilde{\boldsymbol{B}}$ is defined by the link geometry and by the eigenvectors. Thus, it is constant and can be calculated once at the beginning of the simulation.

Let us express the acceleration of nodes 0,1 and 2 as the sum of the two contributes:

$$\begin{aligned} \boldsymbol{a}_0 &= \boldsymbol{a}_0^I + \boldsymbol{a}_0^{II} \\ \boldsymbol{a}_1 &= \boldsymbol{a}_1^I + \boldsymbol{a}_1^{II} \\ \boldsymbol{a}_2 &= \boldsymbol{a}_2^I + \boldsymbol{a}_2^{II} \end{aligned} \tag{35}$$

The first term represents the contributions of the acceleration for null angular velocity; the second one represents the components due to the angular velocity only. Considering that $\boldsymbol{a}_0^I = \boldsymbol{a}_0$,

$\boldsymbol{a}_1^I = \boldsymbol{a}_0 - (\boldsymbol{P}_1 - \boldsymbol{P}_0) \wedge \boldsymbol{\alpha}$ and $\boldsymbol{a}_2^I = \boldsymbol{a}_0 - (\boldsymbol{P}_2 - \boldsymbol{P}_0) \wedge \boldsymbol{\alpha}$, the nodal accelerations for null angular velocity are

$$\ddot{\boldsymbol{e}}^I = \bar{\boldsymbol{R}}\boldsymbol{U}_r\tilde{\boldsymbol{B}}\begin{bmatrix}\boldsymbol{a}_0\\ \boldsymbol{\alpha}\end{bmatrix} \tag{36}$$

The contribution to the nodal accelerations due to the angular velocity is

$$\ddot{\boldsymbol{e}}^{II} = \bar{\boldsymbol{R}}\bar{\boldsymbol{\Omega}}\boldsymbol{U}_r\tilde{\boldsymbol{B}}\begin{bmatrix}\boldsymbol{0}\\ \boldsymbol{\omega}\end{bmatrix} \tag{37}$$

The matrix $\bar{\boldsymbol{\Omega}}$ contains on its main diagonal the skew-symmetric matrices $\boldsymbol{\Omega}$ given by the components of the angular velocity expressed with respect to the link reference frame. The centripetal contribution has been obtained by applying the relationship $\boldsymbol{\omega} \wedge (\boldsymbol{v}_p - \boldsymbol{v}_o) = \boldsymbol{\omega} \wedge [-(\boldsymbol{P} - \boldsymbol{0}) \wedge \boldsymbol{\omega}]$ to all the nodes of the link.

By adding all the contributions due to the nodal accelerations (eq.s 36 and 37), one obtains:

$$\ddot{\boldsymbol{e}} = \ddot{\boldsymbol{e}}^I + \ddot{\boldsymbol{e}}^{II} = \ddot{\boldsymbol{e}} = \bar{\boldsymbol{R}}\boldsymbol{U}_r\tilde{\boldsymbol{B}}\begin{bmatrix}\boldsymbol{a}_0\\ \boldsymbol{\alpha}\end{bmatrix} + \bar{\boldsymbol{R}}\bar{\boldsymbol{\Omega}}\boldsymbol{U}_r\tilde{\boldsymbol{B}}\begin{bmatrix}\boldsymbol{0}\\ \boldsymbol{\omega}\end{bmatrix} \tag{38}$$

The last equation can be simplified by introducing the matrix $\boldsymbol{B} \stackrel{\text{def}}{=} \begin{bmatrix}\tilde{\boldsymbol{B}}\\ \boldsymbol{0}\end{bmatrix}$. The lower block of $\boldsymbol{B}$ is made of a number of null rows equal to the number of elastic modal coordinates of the link. Moreover it is explicitly assumed that the columns of the eigenvectors matrix $\boldsymbol{U}$ (from left to right) are increasing value of the corresponding eigenvalues.

Note that $\boldsymbol{U}_r\tilde{\boldsymbol{B}}$ can be written as $\boldsymbol{UB}$; thus, eq.s 34 and 38 can be rewritten as:

$$\dot{\boldsymbol{e}} = \bar{\boldsymbol{R}}\boldsymbol{UB}\begin{bmatrix}\boldsymbol{v}_0\\ \boldsymbol{\omega}\end{bmatrix} \tag{39}$$

$$\ddot{\boldsymbol{e}} = \bar{\boldsymbol{R}}\boldsymbol{UB}\begin{bmatrix}\boldsymbol{a}_0\\ \boldsymbol{\alpha}\end{bmatrix} + \bar{\boldsymbol{R}}\bar{\boldsymbol{\Omega}}\boldsymbol{UB}\begin{bmatrix}\boldsymbol{0}\\ \boldsymbol{\omega}\end{bmatrix} \tag{40}$$

From eq. 39, the virtual displacements of the nodes of the ERLS are:

$$\delta\boldsymbol{e} = \bar{\boldsymbol{R}}\boldsymbol{UB}\begin{bmatrix}\delta\boldsymbol{P}_0\\ \delta\boldsymbol{\phi}\end{bmatrix} \tag{41}$$

Eventually, since $\delta\boldsymbol{p} = \delta\boldsymbol{e} + \delta\boldsymbol{u}$ and $\ddot{\boldsymbol{p}} = \ddot{\boldsymbol{e}} + \ddot{\boldsymbol{u}}$, the virtual displacements and the absolute accelerations of the nodes are:

$$\delta\boldsymbol{p} = \bar{\boldsymbol{R}}\boldsymbol{UB}\begin{bmatrix}\delta\boldsymbol{P}_0\\ \delta\boldsymbol{\phi}\end{bmatrix} + \delta\bar{\boldsymbol{R}}\boldsymbol{Uq} + \bar{\boldsymbol{R}}\boldsymbol{U}\delta\boldsymbol{q} \tag{42}$$

$$\ddot{\boldsymbol{p}} = \bar{\boldsymbol{R}}\boldsymbol{UB}\begin{bmatrix}\boldsymbol{a}_0\\ \boldsymbol{\alpha}\end{bmatrix} + \bar{\boldsymbol{R}}\bar{\boldsymbol{\Omega}}\boldsymbol{UB}\begin{bmatrix}\boldsymbol{0}\\ \boldsymbol{\omega}\end{bmatrix} + \ddot{\bar{\boldsymbol{R}}}\boldsymbol{Uq} + 2\dot{\bar{\boldsymbol{R}}}\boldsymbol{U}\dot{\boldsymbol{q}} + \bar{\boldsymbol{R}}\boldsymbol{U}\ddot{\boldsymbol{q}} \tag{43}$$

Let $\mathbf{M}$ be the mass matrix expressed with respect to the local reference frame. The virtual work done by the inertial forces is:

$$\delta W_{inertia} = -\delta\boldsymbol{p}^T\,\bar{\boldsymbol{R}}\boldsymbol{M}\bar{\boldsymbol{R}}^T\,\ddot{\boldsymbol{p}} \tag{44}$$

or, introducing eq.s 42 and 43:

$$\delta W_{inertia} = -(\delta \boldsymbol{q}^T \boldsymbol{U}^T + \boldsymbol{q}^T \boldsymbol{U}^T \delta \bar{\boldsymbol{R}}^T \bar{\boldsymbol{R}} + \begin{bmatrix} \delta \boldsymbol{P}_0 \\ \delta \boldsymbol{\phi} \end{bmatrix}^T \boldsymbol{B}^T \boldsymbol{U}^T) \boldsymbol{M}$$
$$(\boldsymbol{U}\boldsymbol{B} \begin{bmatrix} \boldsymbol{a}_0 \\ \boldsymbol{\alpha} \end{bmatrix} + \bar{\boldsymbol{\Omega}} \boldsymbol{U}\boldsymbol{B} \begin{bmatrix} \boldsymbol{0} \\ \boldsymbol{\omega} \end{bmatrix} + \bar{\boldsymbol{R}}^T \ddot{\bar{\boldsymbol{R}}} \boldsymbol{U}\boldsymbol{q} + 2\bar{\boldsymbol{R}}^T \dot{\bar{\boldsymbol{R}}} \boldsymbol{U}\dot{\boldsymbol{q}} + \boldsymbol{U}\ddot{\boldsymbol{q}}) \tag{45}$$

The terms $\delta \bar{\boldsymbol{R}}^T \bar{\boldsymbol{R}}$, $\bar{\boldsymbol{R}}^T \dot{\bar{\boldsymbol{R}}}$ and $\bar{\boldsymbol{R}}^T \ddot{\bar{\boldsymbol{R}}}$ can be written as (see Appendix B):

$$\delta \bar{\boldsymbol{R}}^T \bar{\boldsymbol{R}} = \delta \bar{\boldsymbol{\Phi}}^T \bar{\boldsymbol{R}}^T \dot{\bar{\boldsymbol{R}}} = \bar{\boldsymbol{\Omega}} \text{ and } \bar{\boldsymbol{R}}^T \ddot{\bar{\boldsymbol{R}}} = \bar{\boldsymbol{A}} - \bar{\boldsymbol{\Omega}}^T \bar{\boldsymbol{\Omega}} \tag{46}$$

where:

$$\boldsymbol{\Omega} \stackrel{\text{def}}{=} \begin{bmatrix} 0 & -\omega_z & \omega_y \\ \omega_z & 0 & -\omega_x \\ -\omega_y & \omega_x & 0 \end{bmatrix}, \boldsymbol{A} \stackrel{\text{def}}{=} \begin{bmatrix} 0 & -\alpha_z & \alpha_y \\ \alpha_z & 0 & -\alpha_x \\ -\alpha_y & \alpha_x & 0 \end{bmatrix} \text{ and } \delta\boldsymbol{\Phi} \stackrel{\text{def}}{=} \begin{bmatrix} 0 & -\delta\phi_z & \delta\phi_y \\ \delta\phi_z & 0 & -\delta\phi_x \\ -\delta\phi_y & \delta\phi_x & 0 \end{bmatrix} \tag{47}$$

$\delta\phi_x$,$\delta\phi_y$and $\delta\phi_z$ are the virtual rotational displacements of the link. Using eq.s 46, the virtual work of inertial forces given by (45) can be simplified:

$$\delta W_{inertia} = -(\delta \boldsymbol{q}^T \boldsymbol{U}^T + \boldsymbol{q}^T \boldsymbol{U}^T \delta \bar{\boldsymbol{\Phi}}^T + \begin{bmatrix} \delta \boldsymbol{P}_0 \\ \delta \boldsymbol{\phi} \end{bmatrix}^T \boldsymbol{B}^T \boldsymbol{U}^T) \boldsymbol{M}$$
$$(\boldsymbol{U}\boldsymbol{B} \begin{bmatrix} \boldsymbol{a}_0 \\ \boldsymbol{\alpha} \end{bmatrix} + \bar{\boldsymbol{\Omega}} \boldsymbol{U}\boldsymbol{B} \begin{bmatrix} \boldsymbol{0} \\ \boldsymbol{\omega} \end{bmatrix} + (\bar{\boldsymbol{A}} - \bar{\boldsymbol{\Omega}}^T \bar{\boldsymbol{\Omega}}) \boldsymbol{U}\boldsymbol{q} + 2\bar{\boldsymbol{\Omega}} \boldsymbol{U}\dot{\boldsymbol{q}} + \boldsymbol{U}\ddot{\boldsymbol{q}}) \tag{48}$$

By computing the products between the virtual displacements and the inertial forces, one obtains:

$$\begin{aligned} -\delta W_{inertia} = {} & \delta \boldsymbol{q}^T \boldsymbol{U}^T \boldsymbol{M}\boldsymbol{U}\boldsymbol{B} \begin{bmatrix} \boldsymbol{a}_0 \\ \boldsymbol{\alpha} \end{bmatrix} + \boldsymbol{q}^T \boldsymbol{U}^T \delta \bar{\boldsymbol{\Phi}}^T \boldsymbol{M}\boldsymbol{U}\boldsymbol{B} \begin{bmatrix} \boldsymbol{a}_0 \\ \boldsymbol{\alpha} \end{bmatrix} + \begin{bmatrix} \delta \boldsymbol{P}_0 \\ \delta \boldsymbol{\phi} \end{bmatrix}^T \boldsymbol{B}^T \boldsymbol{U}^T \boldsymbol{M}\boldsymbol{U}\boldsymbol{B} \begin{bmatrix} \boldsymbol{a}_0 \\ \boldsymbol{\alpha} \end{bmatrix} \\ & + \delta \boldsymbol{q}^T \boldsymbol{U}^T \boldsymbol{M}\bar{\boldsymbol{\Omega}}\boldsymbol{U}\boldsymbol{B} \begin{bmatrix} \boldsymbol{0} \\ \boldsymbol{\omega} \end{bmatrix} + \boldsymbol{q}^T \boldsymbol{U}^T \delta \bar{\boldsymbol{\Phi}}^T \boldsymbol{M}\bar{\boldsymbol{\Omega}}\boldsymbol{U}\boldsymbol{B} \begin{bmatrix} \boldsymbol{0} \\ \boldsymbol{\omega} \end{bmatrix} + \begin{bmatrix} \delta \boldsymbol{P}_0 \\ \delta \boldsymbol{\phi} \end{bmatrix}^T \boldsymbol{B}^T \boldsymbol{U}^T \boldsymbol{M}\bar{\boldsymbol{\Omega}}\boldsymbol{U}\boldsymbol{B} \begin{bmatrix} \boldsymbol{0} \\ \boldsymbol{\omega} \end{bmatrix} \\ & + \delta \boldsymbol{q}^T \boldsymbol{U}^T \boldsymbol{M}(\bar{\boldsymbol{A}} - \bar{\boldsymbol{\Omega}}^T \bar{\boldsymbol{\Omega}})\boldsymbol{U}\boldsymbol{q} + \boldsymbol{q}^T \boldsymbol{U}^T \delta \bar{\boldsymbol{\Phi}}^T \boldsymbol{M}(\bar{\boldsymbol{A}} - \bar{\boldsymbol{\Omega}}^T \bar{\boldsymbol{\Omega}})\boldsymbol{U}\boldsymbol{q} + \begin{bmatrix} \delta \boldsymbol{P}_0 \\ \delta \boldsymbol{\phi} \end{bmatrix}^T \boldsymbol{B}^T \boldsymbol{U}^T \boldsymbol{M}(\bar{\boldsymbol{A}} - \bar{\boldsymbol{\Omega}}^T \bar{\boldsymbol{\Omega}})\boldsymbol{U}\boldsymbol{q} \\ & + 2\delta \boldsymbol{q}^T \boldsymbol{U}^T \boldsymbol{M}\bar{\boldsymbol{\Omega}}\boldsymbol{U}\dot{\boldsymbol{q}} + 2\boldsymbol{q}^T \boldsymbol{U}^T \delta \bar{\boldsymbol{\Phi}}^T \boldsymbol{M}\bar{\boldsymbol{\Omega}}\boldsymbol{U}\dot{\boldsymbol{q}} + 2\begin{bmatrix} \delta \boldsymbol{P}_0 \\ \delta \boldsymbol{\phi} \end{bmatrix}^T \boldsymbol{B}^T \boldsymbol{U}^T \boldsymbol{M}\bar{\boldsymbol{\Omega}}\boldsymbol{U}\dot{\boldsymbol{q}} \\ & + \delta \boldsymbol{q}^T \boldsymbol{U}^T \boldsymbol{M}\boldsymbol{U}\ddot{\boldsymbol{q}} + \boldsymbol{q}^T \boldsymbol{U}^T \delta \bar{\boldsymbol{\Phi}}^T \boldsymbol{M}\boldsymbol{U}\ddot{\boldsymbol{q}} + \begin{bmatrix} \delta \boldsymbol{P}_0 \\ \delta \boldsymbol{\phi} \end{bmatrix}^T \boldsymbol{B}^T \boldsymbol{U}^T \boldsymbol{M}\boldsymbol{U}\ddot{\boldsymbol{q}} \end{aligned} \tag{49}$$

Now the virtual work can be split into two sections $\delta W_{inertia} = \delta W^I_{inertia} + \delta W^{II}_{inertia}$, the former containing all the terms related to the second derivative of the variables, the latter containing all the remaining terms.

$$\begin{aligned} -\delta W^I_{inertia} = {} & \delta \boldsymbol{q}^T \boldsymbol{U}^T \boldsymbol{M}\boldsymbol{U}\boldsymbol{B} \begin{bmatrix} \boldsymbol{a}_0 \\ \boldsymbol{\alpha} \end{bmatrix} + \boldsymbol{q}^T \boldsymbol{U}^T \delta \bar{\boldsymbol{\Phi}}^T \boldsymbol{M}\boldsymbol{U}\boldsymbol{B} \begin{bmatrix} \boldsymbol{a}_0 \\ \boldsymbol{\alpha} \end{bmatrix} + \begin{bmatrix} \delta \boldsymbol{P}_0 \\ \delta \boldsymbol{\phi} \end{bmatrix}^T \boldsymbol{B}^T \boldsymbol{U}^T \boldsymbol{M}\boldsymbol{U}\boldsymbol{B} \begin{bmatrix} \boldsymbol{a}_0 \\ \boldsymbol{\alpha} \end{bmatrix} \\ & + \delta \boldsymbol{q}^T \boldsymbol{U}^T \boldsymbol{M}\bar{\boldsymbol{A}}\boldsymbol{U}\boldsymbol{q} + \boldsymbol{q}^T \boldsymbol{U}^T \delta \bar{\boldsymbol{\Phi}}^T \boldsymbol{M}\bar{\boldsymbol{A}}\boldsymbol{U}\boldsymbol{q} + \begin{bmatrix} \delta \boldsymbol{P}_0 \\ \delta \boldsymbol{\phi} \end{bmatrix}^T \boldsymbol{B}^T \boldsymbol{U}^T \boldsymbol{M}\bar{\boldsymbol{A}}\boldsymbol{U}\boldsymbol{q} \\ & + \delta \boldsymbol{q}^T \boldsymbol{U}^T \boldsymbol{M}\boldsymbol{U}\ddot{\boldsymbol{q}} + \boldsymbol{q}^T \boldsymbol{U}^T \delta \bar{\boldsymbol{\Phi}}^T \boldsymbol{M}\boldsymbol{U}\ddot{\boldsymbol{q}} + \begin{bmatrix} \delta \boldsymbol{P}_0 \\ \delta \boldsymbol{\phi} \end{bmatrix}^T \boldsymbol{B}^T \boldsymbol{U}^T \boldsymbol{M}\boldsymbol{U}\ddot{\boldsymbol{q}} \end{aligned} \tag{50}$$

$$\delta W^{II}_{inertia} = -\delta \boldsymbol{q}^T \boldsymbol{U}^T \boldsymbol{M}\bar{\boldsymbol{\Omega}}\boldsymbol{U}\boldsymbol{B}\begin{bmatrix}\boldsymbol{0}\\ \boldsymbol{\omega}\end{bmatrix} - \boldsymbol{q}^T \boldsymbol{U}^T \delta\bar{\boldsymbol{\Phi}}^T \boldsymbol{M}\bar{\boldsymbol{\Omega}}\boldsymbol{U}\boldsymbol{B}\begin{bmatrix}\boldsymbol{0}\\ \boldsymbol{\omega}\end{bmatrix} - \begin{bmatrix}\delta\boldsymbol{P}_0\\ \delta\boldsymbol{\phi}\end{bmatrix}^T \boldsymbol{B}^T \boldsymbol{U}^T \boldsymbol{M}\bar{\boldsymbol{\Omega}}\boldsymbol{U}\boldsymbol{B}\begin{bmatrix}\boldsymbol{0}\\ \boldsymbol{\omega}\end{bmatrix}$$
$$+\delta \boldsymbol{q}^T \boldsymbol{U}^T \boldsymbol{M}\bar{\boldsymbol{\Omega}}^T \bar{\boldsymbol{\Omega}}\boldsymbol{U}\boldsymbol{q} + \boldsymbol{q}^T \boldsymbol{U}^T \delta\bar{\boldsymbol{\Phi}}^T \boldsymbol{M}\bar{\boldsymbol{\Omega}}^T \bar{\boldsymbol{\Omega}}\boldsymbol{U}\boldsymbol{q} + \begin{bmatrix}\delta\boldsymbol{P}_0\\ \delta\boldsymbol{\phi}\end{bmatrix}^T \boldsymbol{B}^T \boldsymbol{U}^T \boldsymbol{M}\bar{\boldsymbol{\Omega}}^T \bar{\boldsymbol{\Omega}}\boldsymbol{U}\boldsymbol{q} \tag{51}$$
$$-2\delta \boldsymbol{q}^T \boldsymbol{U}^T \boldsymbol{M}\bar{\boldsymbol{\Omega}}\boldsymbol{U}\dot{\boldsymbol{q}} - 2\boldsymbol{q}^T \boldsymbol{U}^T \delta\bar{\boldsymbol{\Phi}}^T \boldsymbol{M}\bar{\boldsymbol{\Omega}}\boldsymbol{U}\dot{\boldsymbol{q}} - 2\begin{bmatrix}\delta\boldsymbol{P}_0\\ \delta\boldsymbol{\phi}\end{bmatrix}^T \boldsymbol{B}^T \boldsymbol{U}^T \boldsymbol{M}\bar{\boldsymbol{\Omega}}\boldsymbol{U}\dot{\boldsymbol{q}}$$

The single terms of the last two eq.s are developed in Appendix C.

4.2. Variation of elastic energy for a single link

The elastic energy of a link is given by $\boldsymbol{H} = \frac{1}{2}\boldsymbol{u}^T \boldsymbol{K}\boldsymbol{u}$. Therefore its variation is:

$$\delta \boldsymbol{H} = \delta \boldsymbol{u}^T \boldsymbol{K}\boldsymbol{u} \tag{52}$$

Since $\boldsymbol{u} = \boldsymbol{U}\boldsymbol{q}$, the variation of elastic energy becomes:

$$\delta \boldsymbol{H} = \delta \boldsymbol{q}^T \boldsymbol{U}^T \boldsymbol{K}\boldsymbol{U}\boldsymbol{q} = \delta \boldsymbol{q}^T \boldsymbol{\Gamma}\boldsymbol{q} \tag{53}$$

where the matrix $\boldsymbol{\Gamma}$is a diagonal matrix whose components are the squares of the natural frequencies. Considering just the submatrix $\boldsymbol{\Gamma}_d$ corresponding to the non null eigenvalues, it is possible to write:

$$\delta \boldsymbol{H} = \delta \boldsymbol{q}_d^T \boldsymbol{\Gamma}_d \boldsymbol{q}_d \tag{54}$$

4.3. Virtual work of gravity forces related to a single link

The virtual work done by the gravity forces is:

$$\delta W_g = \delta \boldsymbol{p}^T \boldsymbol{f}_g \tag{55}$$

where $\boldsymbol{f}_g$ are the gravity forces. The virtual displacements can be written as:

$$\delta \boldsymbol{p} = \bar{\boldsymbol{R}}\boldsymbol{U}\boldsymbol{B}\begin{bmatrix}\delta\boldsymbol{P}_0\\ \delta\boldsymbol{\phi}\end{bmatrix} + \delta\bar{\boldsymbol{R}}\boldsymbol{U}\boldsymbol{q} + \bar{\boldsymbol{R}}\boldsymbol{U}\delta\boldsymbol{q} \tag{56}$$

and the gravity forces as:

$$\boldsymbol{f}_g = \bar{\boldsymbol{R}}\boldsymbol{M}\hat{\boldsymbol{g}}_l = \bar{\boldsymbol{R}}\boldsymbol{M}(\hat{\boldsymbol{i}}_1 g_x + \hat{\boldsymbol{i}}_2 g_y + \hat{\boldsymbol{i}}_3 g_z) = \bar{\boldsymbol{R}}\boldsymbol{M}\hat{\boldsymbol{I}}\boldsymbol{g}_l \tag{57}$$

where $\boldsymbol{g}_l = \left\{g_x, g_y, g_z\right\}^T$ represents the gravity expressed with respect to the link's frame. Vectors $\hat{\boldsymbol{i}}_i$ are defined depending on the nature of the nodes (See Appendix D).

Replacing eq. 56 and 57 into 55, produces:

$$\delta W_g = (\begin{bmatrix}\delta\boldsymbol{P}_0\\ \delta\boldsymbol{\phi}\end{bmatrix}^T \boldsymbol{B}^T \boldsymbol{U}^T \bar{\boldsymbol{R}}^T + \boldsymbol{q}^T \boldsymbol{U}^T \delta\bar{\boldsymbol{R}}^T + \delta\boldsymbol{q}^T \boldsymbol{U}^T \bar{\boldsymbol{R}}^T)\bar{\boldsymbol{R}}\boldsymbol{M}\hat{\boldsymbol{I}}\boldsymbol{g}_l \tag{58}$$

or:

$$\delta W_g = \begin{bmatrix}\delta\boldsymbol{P}_0\\ \delta\boldsymbol{\phi}\end{bmatrix}^T \boldsymbol{B}^T \boldsymbol{U}^T \boldsymbol{M}\hat{\boldsymbol{I}}\boldsymbol{g}_l + \boldsymbol{q}^T \boldsymbol{U}^T \delta\bar{\boldsymbol{\Phi}}^T \boldsymbol{M}\hat{\boldsymbol{I}}\boldsymbol{g}_l + \delta\boldsymbol{q}^T \boldsymbol{U}^T \boldsymbol{M}\hat{\boldsymbol{I}}\boldsymbol{g}_l \tag{59}$$

The first term of eq. 59 can be written as:

$$\begin{bmatrix}\delta \boldsymbol{P}_0\\ \delta\boldsymbol{\phi}\end{bmatrix}^T \boldsymbol{B}^T\boldsymbol{U}^T\boldsymbol{M}\hat{\boldsymbol{I}}\boldsymbol{g}_l = \begin{bmatrix}\delta \boldsymbol{P}_0\\ \delta\boldsymbol{\phi}\end{bmatrix}^T \boldsymbol{B}^T\boldsymbol{Q}_4\boldsymbol{g}_l \tag{60}$$

where:

$$\boldsymbol{Q}_4 = \boldsymbol{U}^T\boldsymbol{M}\hat{\boldsymbol{I}} \tag{61}$$

Part of the second term can be written as:

$$\begin{aligned}\boldsymbol{U}^T\delta\bar{\boldsymbol{\Phi}}^T\boldsymbol{M}\hat{\boldsymbol{I}} &= \boldsymbol{U}^T\left(\delta\phi_x\bar{\boldsymbol{A}}_1^T + \delta\phi_y\bar{\boldsymbol{A}}_2^T + \delta\phi_z\bar{\boldsymbol{A}}_3^T\right)\boldsymbol{M}\hat{\boldsymbol{I}}\\ &= \delta\phi_1\boldsymbol{Q}_1 + \delta\phi_2\boldsymbol{Q}_2 + \delta\phi_3\boldsymbol{Q}_3\end{aligned} \tag{62}$$

where: $\boldsymbol{Q}_1 \stackrel{\text{def}}{=} \boldsymbol{U}^T\bar{\boldsymbol{A}}_1^T\boldsymbol{M}\hat{\boldsymbol{I}}$, $\boldsymbol{Q}_2 \stackrel{\text{def}}{=} \boldsymbol{U}^T\bar{\boldsymbol{A}}_2^T\boldsymbol{M}\hat{\boldsymbol{I}}$ and $\boldsymbol{Q}_3 \stackrel{\text{def}}{=} \boldsymbol{U}^T\bar{\boldsymbol{A}}_3^T\boldsymbol{M}\hat{\boldsymbol{I}}$.

The third term can be written as:

$$\delta\boldsymbol{q}^T\boldsymbol{U}^T\boldsymbol{M}\hat{\boldsymbol{I}}\boldsymbol{g}_l = \delta\boldsymbol{q}^T\boldsymbol{Q}_4\boldsymbol{g}_l \tag{63}$$

4.4. Virtual work of the resultant generalized forces (forces or torques) acting on the link

The virtual work done by a generalized force $\boldsymbol{f}$ is:

$$\delta W_f = \delta\boldsymbol{p}^T\boldsymbol{f} \tag{64}$$

where the virtual displacement is:

$$\delta\boldsymbol{p} = \boldsymbol{T}\hat{\boldsymbol{U}}_f\boldsymbol{B}\begin{bmatrix}\delta \boldsymbol{P}_0\\ \delta\boldsymbol{\phi}\end{bmatrix} + \delta\boldsymbol{T}\hat{\boldsymbol{U}}_f\boldsymbol{q} + \boldsymbol{T}\hat{\boldsymbol{U}}_f\delta\boldsymbol{q} \tag{65}$$

In this case $\hat{\boldsymbol{U}}_f$ is a submatrix of $\boldsymbol{U}$. Its rows are the rows of $\boldsymbol{U}$ related to the DoFs the generalized force is applied to.

Let us define the generalized force vector whose components are referred to the local link's reference as $\boldsymbol{f}_l$. The relationship: $\boldsymbol{f} = \boldsymbol{T}\boldsymbol{f}_l$ holds true. Therefore the virtual work done by a generalized force can be written as:

$$\delta W_f = (\begin{bmatrix}\delta \boldsymbol{P}_0\\ \delta\boldsymbol{\phi}\end{bmatrix}^T \boldsymbol{B}^T\hat{\boldsymbol{U}}_f^T\boldsymbol{R}^T + \boldsymbol{q}^T\hat{\boldsymbol{U}}_f^T\delta\boldsymbol{R}^T + \delta\boldsymbol{q}^T\hat{\boldsymbol{U}}_f^T\boldsymbol{R}^T)\boldsymbol{T}\boldsymbol{f}_l \tag{66}$$

or

$$\delta W_f = \begin{bmatrix}\delta \boldsymbol{P}_0\\ \delta\boldsymbol{\phi}\end{bmatrix}^T \boldsymbol{B}^T\hat{\boldsymbol{U}}_f^T\boldsymbol{f}_l + \boldsymbol{q}^T\hat{\boldsymbol{U}}_f^T\delta\boldsymbol{\Phi}^T\boldsymbol{f}_l + \delta\boldsymbol{q}^T\hat{\boldsymbol{U}}_f^T\boldsymbol{f}_l \tag{67}$$

According to (47), the second term of (67) has the following form:

$$\begin{gathered}\boldsymbol{q}^T\hat{\boldsymbol{U}}_f^T\delta\boldsymbol{\Phi}^T\boldsymbol{f}_l =\\ \delta\phi_1\boldsymbol{q}^T\hat{\boldsymbol{U}}_f^T\begin{bmatrix}0&0&0\\0&0&1\\0&-1&0\end{bmatrix}\boldsymbol{f}_l + \delta\phi_2\boldsymbol{q}^T\hat{\boldsymbol{U}}_f^T\begin{bmatrix}0&0&-1\\0&0&0\\1&0&0\end{bmatrix}\boldsymbol{f}_l + \delta\phi_3\boldsymbol{q}^T\hat{\boldsymbol{U}}_f^T\begin{bmatrix}0&1&0\\-1&0&0\\0&0&0\end{bmatrix}\boldsymbol{f}_l\end{gathered} \tag{68}$$

5. Equations of motion

When dealing with a multi-body system, the obtained formulation should be managed to obtain compact motion equations expressed in terms of the accelerations of the DoFs of the system.

Thus, by exploiting eq.s 11, 15 and 24, the virtual terms of the generic $i-th$ link can be rewritten as:

$$\begin{bmatrix} \delta \boldsymbol{P}_{0i} \\ \delta \boldsymbol{\phi}_i \\ \delta \boldsymbol{q} \end{bmatrix} = \begin{bmatrix} \boldsymbol{V}_{\theta i} & \boldsymbol{0} \\ \boldsymbol{0} & \boldsymbol{V}_{qi} \end{bmatrix} \begin{bmatrix} \boldsymbol{J}(\boldsymbol{\theta}) & \boldsymbol{0} \\ \boldsymbol{G}(\boldsymbol{\theta}, \boldsymbol{q}) & \boldsymbol{D}(\boldsymbol{\theta}) \\ \boldsymbol{0} & \boldsymbol{I} \end{bmatrix} \begin{bmatrix} \delta \boldsymbol{\theta} \\ \delta \boldsymbol{q}_d \end{bmatrix} = \boldsymbol{V}_i^o \boldsymbol{N} \begin{bmatrix} \delta \boldsymbol{\theta} \\ \delta \boldsymbol{q}_d \end{bmatrix} \tag{69}$$

where $\boldsymbol{J}(\boldsymbol{\theta})$ represents the Jacobian matrix of the ERLS, and the $\boldsymbol{V}_i^o$ a selection matrix for the proper elements of the $i-th$ link. The $\boldsymbol{V}_i^o$ matrix is block diagonal and allows to select the correct terms related both to the rigid DoFs and to the independent vibration modal coordinates.

Also the acceleration terms can be rewritten as function of the independent variables:

$$\begin{bmatrix} \boldsymbol{a}_{0i} \\ \boldsymbol{\alpha}_i \\ \ddot{\boldsymbol{q}} \end{bmatrix} = \boldsymbol{V}_i^o \boldsymbol{N} \begin{bmatrix} \ddot{\boldsymbol{\theta}} \\ \ddot{\boldsymbol{q}}_{\boldsymbol{d}} \end{bmatrix} + \boldsymbol{V}_i^o \begin{bmatrix} \dot{\boldsymbol{J}}(\boldsymbol{\theta}, \dot{\boldsymbol{\theta}})\dot{\boldsymbol{\theta}} \\ \boldsymbol{n}(\boldsymbol{\theta}, \dot{\boldsymbol{\theta}}, \boldsymbol{q}, \dot{\boldsymbol{q}}) \\ \boldsymbol{0} \end{bmatrix} \tag{70}$$

where $\dot{\boldsymbol{J}}(\boldsymbol{\theta}, \dot{\boldsymbol{\theta}})$ represents the first time derivative of the Jacobian matrix of the ERLS; the second term of the equation depends only on the position and velocity of the independent variables and is thus known.

In such a way, all the terms of the $i-th$ link are expressed as functions of the independent variables and can be easily added and computed.

The virtual work done by the inertial forces $\delta W^I_{inertia,i}$ and $\delta W^{II}_{inertia,i}$ of each link, and the virtual works done by the gravitational δW_g and generalized δW_f forces, can be reformulated in a more compact form. Namely, by gathering in the $\mathbf{L}_i$ matrix all the terms not depending on the virtual displacements and accelerations, the contribution given by $\delta W^I_{inertia,i}$ becomes:

$$-\delta W^I_{inertia,i} = \begin{bmatrix} \delta \boldsymbol{P}_{0i}^T & \delta \boldsymbol{\phi}_i^T & \delta \boldsymbol{q}^T \end{bmatrix} \boldsymbol{L}_i \begin{bmatrix} \boldsymbol{a}_{0i} \\ \boldsymbol{\alpha}_i \\ \ddot{\boldsymbol{q}} \end{bmatrix} \tag{71}$$

Now, by substituting eq. 69 and eq. 70, it holds:

$$-\delta W^I_{inertia,i} = \begin{bmatrix} \delta \boldsymbol{\theta}^T & \delta \boldsymbol{q}_d^T \end{bmatrix} \boldsymbol{N}^T \boldsymbol{V}_i^{oT} \boldsymbol{L}_i (\boldsymbol{V}_i^o \boldsymbol{N} \begin{bmatrix} \ddot{\boldsymbol{\theta}} \\ \ddot{\boldsymbol{q}}_{\boldsymbol{d}} \end{bmatrix} + \boldsymbol{V}_i^o \begin{bmatrix} \dot{\boldsymbol{J}}(\boldsymbol{\theta}, \dot{\boldsymbol{\theta}})\dot{\boldsymbol{\theta}} \\ \boldsymbol{n}(\boldsymbol{\theta}, \dot{\boldsymbol{\theta}}, \boldsymbol{q}, \dot{\boldsymbol{q}}) \\ \boldsymbol{0} \end{bmatrix}) \tag{72}$$

The $\delta W^{II}_{inertia,i}$ term can be expressed by gathering in the $\boldsymbol{l}_i$ matrix all the terms not depending on the virtual displacements:

$$\delta W^{II}_{inertia,i} = \begin{bmatrix} \delta \boldsymbol{P}_{0i}^T & \delta \boldsymbol{\phi}_i^T & \delta \boldsymbol{q}^T \end{bmatrix} \boldsymbol{l}_i = \begin{bmatrix} \delta \boldsymbol{\theta}^T & \delta \boldsymbol{q}_d^T \end{bmatrix} \boldsymbol{N}^T \boldsymbol{V}_i^{oT} \boldsymbol{l}_i \tag{73}$$

Now, since the second term in eq. 72 does not eventually depend on the virtual displacements, it can be included in the $\boldsymbol{l}_i$ matrix.

All the other terms, i.e. the variation of the elastic energy $\delta \boldsymbol{H}$ (eq.54), of the gravity forces δW_g (eq. 60, 62 and 63), and of the resultant generalized forces δW_f (eq.67) do not depend on

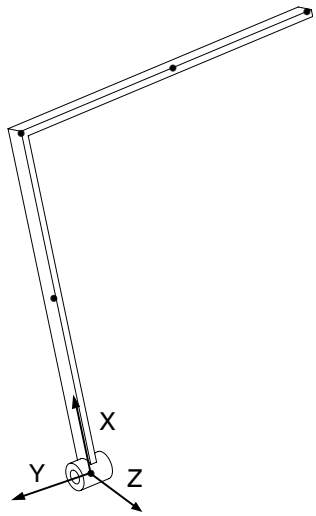

Figure 2: L-shaped mechanism: reference frame and node discretization

accelerations and can be gathered into the right hand term of the dynamic system equation; for sake of clarity, the matrix $\boldsymbol{l}$ which now includes all these contributes will be named $\tilde{\boldsymbol{l}}_{\boldsymbol{i}}$. By naming δW_i the term which includes all the contributions not depending on accelerations, we obtain:

$$\delta W_i = \begin{bmatrix} \delta \boldsymbol{P}_{0i}^T & \delta \boldsymbol{\phi}_i^T & \delta \boldsymbol{q}^T \end{bmatrix} \tilde{\boldsymbol{l}}_{\boldsymbol{i}} = \begin{bmatrix} \delta \boldsymbol{\theta}^T & \delta \boldsymbol{q}_d^T \end{bmatrix} \boldsymbol{N}^T \boldsymbol{V}_i^{oT} \tilde{\boldsymbol{l}}_{\boldsymbol{i}} \tag{74}$$

By adding up all the links contributions, the following equation is obtained:

$$-\delta W_{inertia}^I = \sum_{i=1}^{N} \begin{bmatrix} \delta \boldsymbol{\theta}^T & \delta \boldsymbol{q}_d^T \end{bmatrix} \boldsymbol{N}^T \boldsymbol{V}_i^{oT} \boldsymbol{L}_i (\boldsymbol{V}_i^o \boldsymbol{N} \begin{bmatrix} \ddot{\boldsymbol{\theta}} \\ \ddot{\boldsymbol{q}}_{\boldsymbol{d}} \end{bmatrix} + \boldsymbol{V}_i^o \begin{bmatrix} \dot{\boldsymbol{J}}(\boldsymbol{\theta}, \dot{\boldsymbol{\theta}}) \dot{\boldsymbol{\theta}} \\ \boldsymbol{n}(\boldsymbol{\theta}, \dot{\boldsymbol{\theta}}, \boldsymbol{q}, \dot{\boldsymbol{q}}) \\ \boldsymbol{0} \end{bmatrix}) =$$

$$= \delta W = \sum_{i=1}^{N} \begin{bmatrix} \delta \boldsymbol{\theta}^T & \delta \boldsymbol{q}_d^T \end{bmatrix} \boldsymbol{N}^T \boldsymbol{V}_i^{oT} \tilde{\boldsymbol{l}}_{\boldsymbol{i}}$$

Finally, by letting $\boldsymbol{L} \stackrel{\text{def}}{=} \sum_{i=1}^{N} \boldsymbol{V}_i^{oT} \boldsymbol{L}_i \boldsymbol{V}_i^o$ and $\tilde{\boldsymbol{l}} \stackrel{\text{def}}{=} \sum_{i=1}^{N} \boldsymbol{V}_i^{oT} \tilde{\boldsymbol{l}}_{\boldsymbol{i}}$, and discarding the virtual displacements, the final model representation is obtained:

$$\boldsymbol{N}^T \boldsymbol{L} \boldsymbol{N} \begin{bmatrix} \ddot{\boldsymbol{\theta}} \\ \ddot{\boldsymbol{q}}_{\boldsymbol{d}} \end{bmatrix} = \boldsymbol{N}^T \left(-\boldsymbol{L} \begin{bmatrix} \dot{\boldsymbol{J}}(\boldsymbol{\theta}, \dot{\boldsymbol{\theta}}) \boldsymbol{\theta} \\ \boldsymbol{n}(\boldsymbol{\theta}, \dot{\boldsymbol{\theta}}, \boldsymbol{q}, \dot{\boldsymbol{q}}) \\ \boldsymbol{0} \end{bmatrix} + \tilde{\boldsymbol{l}} \right) \tag{75}$$

6. Numerical implementation and model validation

A MatLab™ software simulator has been implemented in order to test and to validate the dynamic model presented in the previous Sections. A L-shaped benchmark mechanism has been chosen (Gasparetto et al. 2013), as in Fig. 2. The particular shape of the system has been chosen to allow a 3D motion of the mechanism, i.e. to induce motion and vibrations in different directions, and not only on a plane as often made in literature, see (Dwivedy and Eberhard 2006).

Table 2: Geometrical and mechanical parameters of the L-shaped mechanism

Elem.	Material	Length [m]	Depth [m]	Width [m]	Density ρ [kg/m^3]	Poisson's ratio	Young's m. [N/m^2]
1st	Steel	0.5	0.03	0.01	7800	0.33	2e^{11}
2nd	Steel	0.5	0.03	0.01	7800	0.33	2e^{11}

The results have been compared with those provided by Adams™ for the same mechanism. It is well known that the Adams™ software uses a Floating Frame of Reference approach and a Component Mode Synthesis technique based on the Craig-Bampton method where the DoFs of the system are partitioned into boundary and interior DoFs and the formers are exactly preserved when higher order modes are truncated and the system dimension reduced (Craig and Bampton 1968).

In Adams™, the link flexibility is imported and loaded through a special file, i.e. the modal neutral file. Thus, firstly the links have to be modeled and meshed in a computer-aided engineering simulation software such as Ansys™ and then the proper file generated. For this purpose a special toolbox is available in Ansys™ (ANSYS 2011).

In the ERLS-CMS model under consideration, a similar approach can be used. Indeed, to set up the significant terms of each link such as, for instance, eigenvectors and eigenvalues, the same files based on the Craig-Bampton reduction that Adams™ uses to import the link flexibility can be exploited for the formulation under evaluation. Thus, the comparison can be made being sure that the two approaches work with the same kind of modal reduction.

The L-shaped mechanism chosen for the tests is made of two flexible rods and can be considered as the 3D version of the classic single-link planar mechanism adopted as benchmark in other approaches limited to a 2D motion.

6.1. Test 1: convergence of the solution

In the first numerical test the convergence of the solution of the ERLS-CMS model implemented in Matlab™ has been evaluated; the main geometrical and mechanical parameters of the tested mechanism are reported in Table 2.

Since the L-shaped system can rotate only around its y-axis, i.e. it has one rigid DoF, due to the chosen mechanical and geometrical parameters, small deformations but large rotations are taken into account. In Ansys™ the link has been modeled with four Euler-Bernoulli beams: each beam has two nodes and six degrees of freedom, thus the whole mechanism link has five nodes and thirty eigenvalues. The modal neutral file has been built by choosing as interface nodes the first and last node of the L-shaped mechanism and exporting 18 modes over the 30 available.

The motion is simulated under gravity ($g = 9.81\ m/s^2$), without friction and damping, by releasing the mechanism from the horizontal ($\theta = 0$ deg) position. The chosen solver was a modified Runge–Kutta algorithm. Figures 3(a) and 3(b) show the Z motion of the elbow and of the last node of the L-shaped mechanism with respect to the number of considered modes, respectively. In Table 3, the θ and the 3rd and 5th node coordinates at a specific time, i.e. 0.5 s, are reported. As can be seen from the results, the comparisons show the converge of the solution and the system behavior by changing the number of considered modes.

With a number of 6 modes only the rigid behavior is simulated; by considering more modes, the elastic behaviour is taken into account. By increasing the number of modes, the convergence to the solution obtained through the FFR model can be achieved, as highlighted by the results

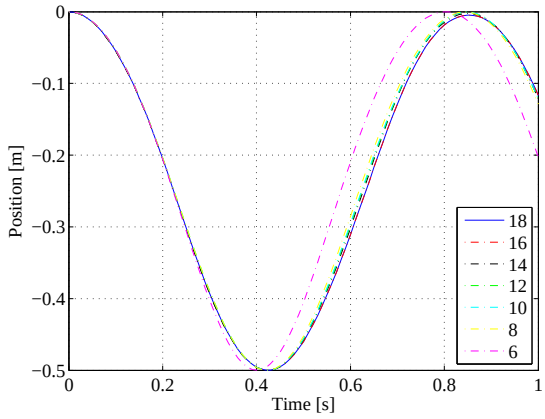

(a)

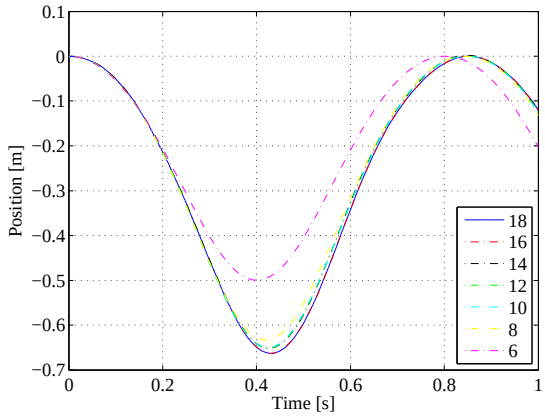

(b)

Figure 3: L-shape mechanism: Z-coordinate of the mechanism elbow (a) and of the mechanism tip (d) with respect to the number of selected modes.

Table 3: Comparison of Θ and the 3rd and 5th node coordinates at t=0.5 [s]

mode N	Θ deg	3rd X-coord [m]	3rd Y-coord [m]	3rd Z-coord [m]	5th X-coord [m]	5th Y-coord [m]	5th Z-coord [m]
6	125.90	-0.2931	0	-0.4050	-0.2931	0	-0.4050
8	115.30	-0.2139	-0.0357	-0.4520	-0.2607	0.4643	-0.5509
10	114.30	-0.2061	-0.0491	-0.4555	-0.2596	0.4509	-0.5735
12	114.25	-0.2044	-0.0500	-0.4563	-0.2615	0.4500	-0.5741
14	114.20	-0.2027	-0.0509	-0.4571	-0.2635	0.4491	-0.5766
16	113.50	-0.1970	-0.0637	-0.4596	-0.2626	0.4491	-0.5955
18	113.50	-0.1970	-0.0637	-0.4596	-0.2626	0.4362	-0.5955

presented in the next section. Anyway, a general rule for the choice of a suitable number of nodes can be made according to the bandwidth of the actuator, by considering that the dynamic model of the flexible system should reproduce with sufficient accuracy all the modes that lie within this limit. This rule, which is commonly applied, is based upon the fact that a mode cannot be excited if it lies beyond the bandwidth of the actuator.

6.2. Test 2: comparison of the ERLS and FFR approaches with respect to the number of considered modes

In order to show the behavior of the ERLS-CMS formulation for a spatial mechanism with respect to the FFR-CMS, a first comparison between the MatLab ™ simulator and the Adams™ software has been performed. The simulation lasts 2 seconds and the L-shaped mechanism has been evaluated under gravity, in absence of frictional forces and damping, starting from a 0 degree condition. The chosen solver was a modified Runge–Kutta algorithm and in a first simulation a modal neutral file with 18 modes has been considered while, in a second simulation, a modal neutral file with all the 30 modes has been used. Adams™ results are presented taking into account all the modes present in the modal neutral file. It should be highlighted that high order modes are included just to show the agreement between the novel dynamical model and the FFR formulation. It is known that analytical models are often incapable of describing with accuracy the behavior of a flexible system at high frequencies.

Figure 4(a) show the Y- coordinate of the last node of the L-shaped mechanism with respect to the number of considered modes, up to 30. In Figure 4(b), a magnification of Figure 4(a) around 1.2 s is shown. It can be seen that the results provided by the ERLS-CMS approach are in good agreement with those given by Adams™ and how the signals overlap almost perfectly.

Regarding the computing time needed to solve the dynamic system, since the two approaches are implemented in different software, i.e. Matlab™ and Adams™ , at the actual stage it is not possible to make a proper comparison between the two. Indeed, as a general consideration, it can be said that, since the ERLS approach is implemented in a non-optimized code, the simulations take comparable computing time in case of a low number of modes while, by adding modes with relative high frequencies, the Adams™ simulation time becomes lower.

By looking at the previous ERLS implementation, since the new formulation allows reducing the number of DoFs of the considered system with respect to the ERLS-FEM approach, the computational time required decreases. Indeed, it is highly dependent on the number of DoFs, now the number of kept modes and their frequency; the choice of the selected modes could be made in different manners and if only the lower frequency modes are maintained, a faster integration time is required for finding the solution of the dynamic system.

6.3. Test 3: comparison of the ERLS and FFR approaches under a torque input command

In order highlight the vibrational behavior of the L-shaped link in terms of frequency and shape of deformation, the mechanism response to a torque input has been simulated and the results compared with Adams™The geometrical and mechanical parameters of the mechanism and the input torque signal have been chosen as in Table 4 and Figure 5 Gasparetto et al. 2013, and the simulation has been performed without any friction ord damping. Extra inertias and a concentrated mass have been introduced in order to take into account the motor, i.e. $I_m = 0.0043 kgm^2$ and shrink disc, i.e. $I_c = 0.001269 kgm^2$, inertias and the elbow articulation mass, i.e. 0.017 kg. The input signal allows, from a statically balanced configuration at 135°, to fast accelerate and decelerate the L-beam, according to the torque profile reported in figure 5.

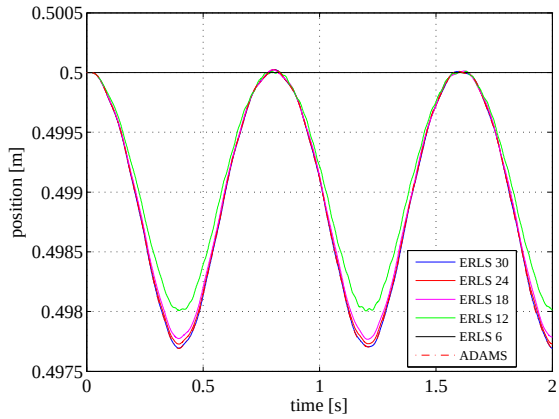

(a)

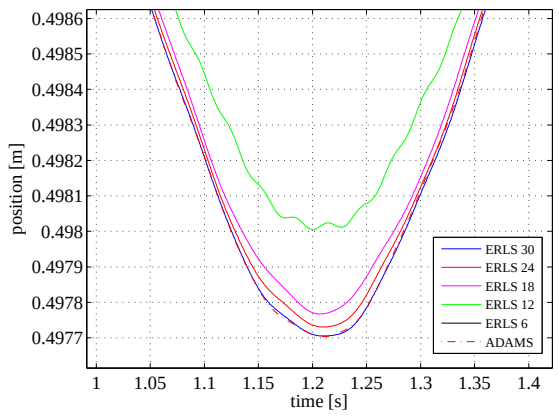

(b)

Figure 4: L-shape mechanism comparison: Y-coordinate of the mechanism tip (a) and its magnification at about t= 1.2 s (b).

Table 4: Geometrical and mechanical parameters of the L-shaped mechanism under an input torque signal

Elem.	Material	Length [m]	Depth [m]	Width [m]	Density ρ [kg/m^3]	Poisson's ratio	Young's m. [N/m^2]
1st	Aluminium	0.5	0.008	0.008	2700	0.33	7e^{10}
2nd	Aluminium	0.5	0.008	0.008	2700	0.33	7e^{10}

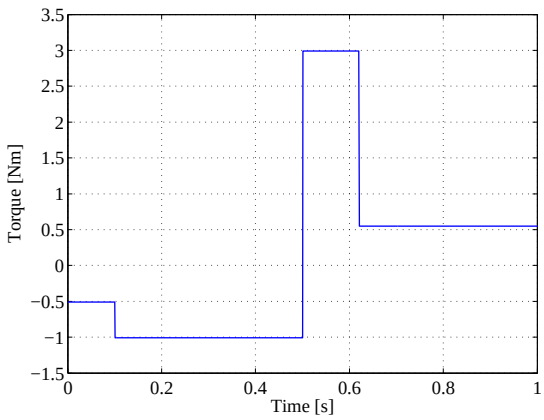

Figure 5: Input torque signal.

As for the previous results, the link has been modeled in Ansys™ with four Euler-Bernoulli beams, the modal neutral file has been built by choosing as interface nodes the first and last node of the L-shaped mechanism and by exporting 18 modes over the 30 available.

Figure 6 shows the elbow Z-coordinate position comparison of the last node of the first part of the L-shape mechanism, i.e. the elbow, between the simulated ERLS-CMS and Adams™ while Figures 7 and 8 show the elbow Z-coordinate acceleration in the time and frequency domain, respectively.

As can be seen in Figure 8, the ERLS-CMS and Adams™ signals match very well each other and the main frequencies of the mechanism under test, i.e. 11, 31, 113, 171 Hz, are captured and properly simulated.

Conclusions and future work

In this paper an Equivalent Rigid Link System (ERLS) formulation is extended with Component Mode Synthesis (CMS) to develop a novel dynamic model of spatial flexible mechanisms. After the definition of the model kinematics, the dynamic equations coupling rigid body and flexible body motion are obtained and discussed.

The model has been implemented and numerically validated by comparing its response with a commercial simulator based on the FFR formulation. The tests, performed both under gravity and under a forced torque input, show a good agreement between the results, thus proving the effectiveness of the proposed dynamic model.

Future work will be devoted to further validate the model through experimental tests both on a L-shape and on another benchmark mechanism with at least two rigid DoFs.

Acknowledgement

This work was partially supported by the Free University of Bolzano internal research funds project TN5043-Development and validation of dynamic models for high-performance manipulators.

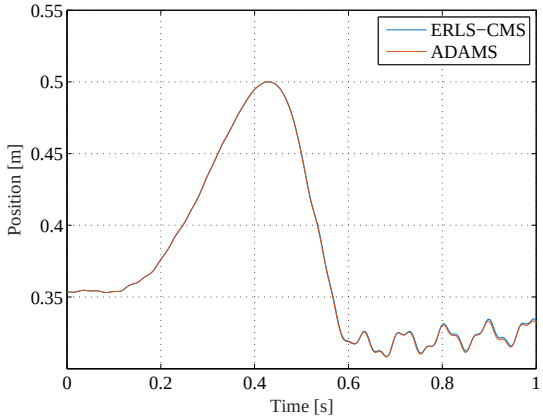

Figure 6: Comparison of the elbow Z-coordinate of the L-shape mechanism under torque input.

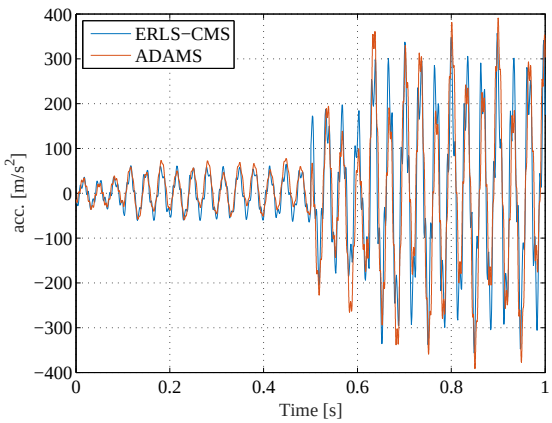

Figure 7: Comparison of the elbow Z-coordinate acceleration of the L-shape mechanism under torque input in the time domain.

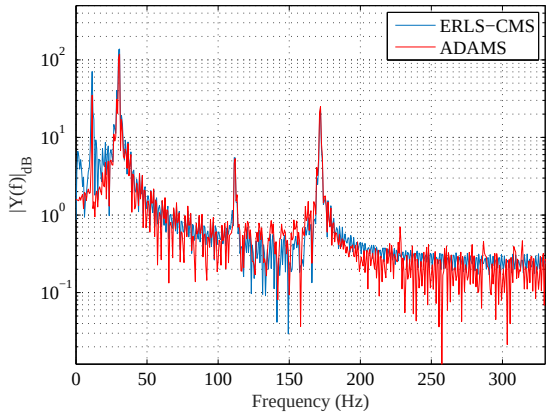

Figure 8: Comparison of the elbow Z-coordinate acceleration of the L-shape mechanism under torque input in the frequency domain.

APPENDIX A: $\hat{B}$ matrix.

Using the skew-symmetric matrix definition $\left[\begin{Bmatrix} a & b & c \end{Bmatrix}^T\right]_X \stackrel{\text{def}}{=} \begin{bmatrix} 0 & -c & b \\ c & 0 & -a \\ -b & a & 0 \end{bmatrix}$ employed for cross product operation,

$$\hat{\boldsymbol{B}} \stackrel{\text{def}}{=} \left[\begin{array}{c|c} \boldsymbol{I} & \boldsymbol{0} \\ \hline \boldsymbol{I} & \left[-(\boldsymbol{P}_1 - \boldsymbol{P}_0)\right]_X \\ \hline \boldsymbol{I} & \left[-(\boldsymbol{P}_2 - \boldsymbol{P}_0)\right]_X \end{array}\right] \tag{.1}$$

APPENDIX B: Development of the terms involving rotational matrices.

Let us find a new formulation for the terms containing the rotational matrix, namely: $\delta\overline{\boldsymbol{R}}^T\overline{\boldsymbol{R}}$, $\overline{\boldsymbol{R}}^T\dot{\overline{\boldsymbol{R}}}$ and $\overline{\boldsymbol{R}}^T\ddot{\overline{\boldsymbol{R}}}$. The following eq.s hold true:

$$\boldsymbol{R}^T\boldsymbol{T} = \boldsymbol{I},\ \boldsymbol{R}^T\dot{\boldsymbol{R}} = \boldsymbol{\Omega} \text{ and } \boldsymbol{R}^T\ddot{\boldsymbol{R}} + \dot{\boldsymbol{R}}^T\dot{\boldsymbol{R}} = \boldsymbol{A} \tag{.2}$$

where:

$$\boldsymbol{\Omega} \stackrel{\text{def}}{=} \begin{bmatrix} 0 & -\omega_z & \omega_y \\ \omega_z & 0 & -\omega_x \\ -\omega_y & \omega_x & 0 \end{bmatrix} \tag{.3}$$

and:

$$\mathbf{A} \stackrel{\text{def}}{=} \begin{bmatrix} 0 & -\alpha_z & \alpha_y \\ \alpha_z & 0 & -\alpha_x \\ -\alpha_y & \alpha_x & 0 \end{bmatrix} \tag{.4}$$

are skew-symmetric matrices referring respectively to the absolute angular velocity and absolute angular acceleration of the link.

Since $\dot{\boldsymbol{R}}^T\dot{\boldsymbol{R}} = \boldsymbol{\Omega}^T\boldsymbol{T}^T\boldsymbol{T}\boldsymbol{\Omega} = \boldsymbol{\Omega}^T\boldsymbol{\Omega}$, it yields $\boldsymbol{R}^T\ddot{\boldsymbol{R}} = \boldsymbol{A} - \boldsymbol{\Omega}^T\boldsymbol{\Omega}$. Moreover $\dot{\boldsymbol{R}} = \boldsymbol{T}\boldsymbol{\Omega}$, and thus, $\delta\boldsymbol{T} = \boldsymbol{T}\delta\boldsymbol{\Phi}$, where:

$$\delta\boldsymbol{\Phi} \stackrel{\text{def}}{=} \begin{bmatrix} 0 & -\delta\phi_z & \delta\phi_y \\ \delta\phi_z & 0 & -\delta\phi_x \\ -\delta\phi_y & \delta\phi_x & 0 \end{bmatrix} \tag{.5}$$

is a skew-symmetric matrix; its components are the virtual rotational displacements expressed with respect to the local frame of the link. By pre-multiplying the previous eq. by $\delta\boldsymbol{T}^T$, one gets:

$$\delta\boldsymbol{T}^T\boldsymbol{T} = \delta\boldsymbol{\Phi}^T\boldsymbol{T}^T\boldsymbol{T} = \delta\boldsymbol{\Phi}^T \tag{.6}$$

In conclusion, extending the results to the matrix $\bar{\boldsymbol{R}}$, which contains on its main diagonal the single rotational matrices referred to each link, one gets:

$$\delta\bar{\boldsymbol{R}}^T\bar{\boldsymbol{R}} = \delta\bar{\boldsymbol{\Phi}}^T, \bar{\boldsymbol{R}}^T\dot{\bar{\boldsymbol{R}}} = \bar{\boldsymbol{\Omega}} \text{ and } \bar{\boldsymbol{R}}^T\ddot{\bar{\boldsymbol{R}}} = \bar{\boldsymbol{A}} - \bar{\boldsymbol{\Omega}}^T\bar{\boldsymbol{\Omega}} \tag{.7}$$

APPENDIX C: Development of the constant inertial matrices related to a single link

The terms related to the inertial matrix of eq. 50 and 51 can be written as:

$$\boldsymbol{U}^T\boldsymbol{M}\bar{\boldsymbol{A}}\boldsymbol{U} = \boldsymbol{U}^T\boldsymbol{M}\left(\alpha_x\bar{\boldsymbol{A}}_1 + \alpha_y\bar{\boldsymbol{A}}_2 + \alpha_z\bar{\boldsymbol{A}}_3\right)\boldsymbol{U} \tag{.8}$$

where: $\boldsymbol{A}_1 \stackrel{\text{def}}{=} \begin{bmatrix} 0 & 0 & 0 \\ 0 & 0 & -1 \\ 0 & 1 & 0 \end{bmatrix}$, $\boldsymbol{A}_2 \stackrel{\text{def}}{=} \begin{bmatrix} 0 & 0 & 1 \\ 0 & 0 & 0 \\ -1 & 0 & 0 \end{bmatrix}$ and $\boldsymbol{A}_3 \stackrel{\text{def}}{=} \begin{bmatrix} 0 & -1 & 0 \\ 1 & 0 & 0 \\ 0 & 0 & 0 \end{bmatrix}$. By introducing the notations: $\boldsymbol{X}_1 = \boldsymbol{U}^T\boldsymbol{M}\bar{\boldsymbol{A}}_1\boldsymbol{U}$, $\boldsymbol{X}_2 = \boldsymbol{U}^T\boldsymbol{M}\bar{\boldsymbol{A}}_2\boldsymbol{U}$, and: $\boldsymbol{X}_3 = \boldsymbol{U}^T\boldsymbol{M}\bar{\boldsymbol{A}}_3\boldsymbol{U}$ eq. .8 becomes:

$$\boldsymbol{U}^T\boldsymbol{M}\bar{\boldsymbol{A}}\boldsymbol{U} = \alpha_x\boldsymbol{X}_1 + \alpha_y\boldsymbol{X}_2 + \alpha_z\boldsymbol{X}_3 \tag{.9}$$

Following the same reasoning, the term $\boldsymbol{U}^T\boldsymbol{M}\bar{\boldsymbol{\Omega}}\boldsymbol{U}$ of eq. 51 can be written as:

$$\boldsymbol{U}^T\boldsymbol{M}\bar{\boldsymbol{\Omega}}\boldsymbol{U} = \omega_x\boldsymbol{X}_1 + \omega_y\boldsymbol{X}_2 + \omega_z\boldsymbol{X}_3 \tag{.10}$$

Moreover, since $\boldsymbol{U}^T\delta\bar{\boldsymbol{\Phi}}^T\boldsymbol{M}\boldsymbol{U} = \left(\boldsymbol{U}^T\boldsymbol{M}\delta\bar{\boldsymbol{\Phi}}\boldsymbol{U}\right)^T$, it yields:

$$\boldsymbol{U}^T\delta\bar{\boldsymbol{\Phi}}^T\boldsymbol{M}\boldsymbol{U} = \delta\phi_x\boldsymbol{X}_1^T + \delta\phi_y\boldsymbol{X}_2^T + \delta\phi_z\boldsymbol{X}_3^T \tag{.11}$$

Note that the product $\boldsymbol{\Omega}^T\boldsymbol{\Omega}$ is:

$$\boldsymbol{\Omega}^T\boldsymbol{\Omega} = \begin{bmatrix} (\omega_y^2 + \omega_z^2) & -\omega_x\omega_y & -\omega_x\omega_z \\ -\omega_x\omega_y & (\omega_x^2 + \omega_z^2) & -\omega_y\omega_z \\ -\omega_x\omega_z & -\omega_y\omega_z & (\omega_x^2 + \omega_y^2) \end{bmatrix} \tag{.12}$$

Thus, it can be written as:

$$\boldsymbol{\Omega}^T\boldsymbol{\Omega} = (\omega_y^2 + \omega_z^2)\boldsymbol{S}_1 + (\omega_x^2 + \omega_z^2)\boldsymbol{S}_2 + (\omega_x^2 + \omega_y^2)\boldsymbol{S}_3 + \omega_x\omega_y\boldsymbol{S}_4 + \omega_x\omega_z\boldsymbol{S}_5 + \omega_y\omega_z\boldsymbol{S}_6 \tag{.13}$$

where: $\boldsymbol{S}_1 \stackrel{\text{def}}{=} \begin{bmatrix} 1 & 0 & 0 \\ 0 & 0 & 0 \\ 0 & 0 & 0 \end{bmatrix}$, $\boldsymbol{S}_2 \stackrel{\text{def}}{=} \begin{bmatrix} 0 & 0 & 0 \\ 0 & 1 & 0 \\ 0 & 0 & 0 \end{bmatrix}$, $\boldsymbol{S}_3 \stackrel{\text{def}}{=} \begin{bmatrix} 0 & 0 & 0 \\ 0 & 0 & 0 \\ 0 & 0 & 1 \end{bmatrix}$, $\boldsymbol{S}_4 \stackrel{\text{def}}{=} \begin{bmatrix} 0 & -1 & 0 \\ -1 & 0 & 0 \\ 0 & 0 & 0 \end{bmatrix}$, $\boldsymbol{S}_5 \stackrel{\text{def}}{=} \begin{bmatrix} 0 & 0 & -1 \\ 0 & 0 & 0 \\ -1 & 0 & 0 \end{bmatrix}$ and $\boldsymbol{S}_6 \stackrel{\text{def}}{=} \begin{bmatrix} 0 & 0 & 0 \\ 0 & 0 & -1 \\ 0 & -1 & 0 \end{bmatrix}$. Now, introducing the variables: $\boldsymbol{Y}_1 \stackrel{\text{def}}{=} \boldsymbol{U}^T \boldsymbol{M}\bar{\boldsymbol{S}}_1\boldsymbol{U}$, $\boldsymbol{Y}_2 \stackrel{\text{def}}{=} \boldsymbol{U}^T \boldsymbol{M}\bar{\boldsymbol{S}}_2\boldsymbol{U}$, $\boldsymbol{Y}_3 \stackrel{\text{def}}{=} \boldsymbol{U}^T \boldsymbol{M}\bar{\boldsymbol{S}}_3\boldsymbol{U}$, $\boldsymbol{Y}_4 \stackrel{\text{def}}{=} \boldsymbol{U}^T \boldsymbol{M}\bar{\boldsymbol{S}}_4\boldsymbol{U}$, $\boldsymbol{Y}_5 \stackrel{\text{def}}{=} \boldsymbol{U}^T \boldsymbol{M}\bar{\boldsymbol{S}}_5\boldsymbol{U}$ and $\boldsymbol{Y}_6 \stackrel{\text{def}}{=} \boldsymbol{U}^T \boldsymbol{M}\bar{\boldsymbol{S}}_6\boldsymbol{U}$, one can write:

$$\boldsymbol{U}^T \boldsymbol{M}\bar{\boldsymbol{\Omega}}^T \bar{\boldsymbol{\Omega}}\boldsymbol{U} = (\omega_y^2 + \omega_z^2)\boldsymbol{Y}_1 + (\omega_x^2 + \omega_z^2)\boldsymbol{Y}_2 + (\omega_x^2 + \omega_y^2)\boldsymbol{Y}_3 + \omega_x\omega_y\boldsymbol{Y}_4 + \omega_x\omega_z\boldsymbol{Y}_5 + \omega_y\omega_z\boldsymbol{Y}_6 \quad (.14)$$

Thanks to the introduction of $\bar{\boldsymbol{A}}_1$, $\bar{\boldsymbol{A}}_3$ and $\bar{\boldsymbol{A}}_3$, the previous equation can be written as:

$$\boldsymbol{U}^T \delta\bar{\boldsymbol{\Phi}}^T \boldsymbol{M}\bar{\boldsymbol{A}}\boldsymbol{U} = \boldsymbol{U}^T \left(\delta\phi_x \bar{\boldsymbol{A}}_1^T + \delta\phi_y \bar{\boldsymbol{A}}_2^T + \delta\phi_z \bar{\boldsymbol{A}}_3^T\right) \boldsymbol{M} \left(\alpha_x \bar{\boldsymbol{A}}_1 + \alpha_y \bar{\boldsymbol{A}}_2 + \alpha_z \bar{\boldsymbol{A}}_3\right) \boldsymbol{U} \quad (.15)$$

and, after multiplications:

$$\begin{aligned} \boldsymbol{U}^T \delta\bar{\boldsymbol{\Phi}}^T \boldsymbol{M}\bar{\boldsymbol{A}}\boldsymbol{U} = {} & \delta\phi_x \left(\alpha_x \boldsymbol{Z}_{11} + \alpha_y \boldsymbol{Z}_{12} + \alpha_z \boldsymbol{Z}_{13}\right) \\ & + \delta\phi_y \left(\alpha_x \boldsymbol{Z}_{21} + \alpha_y \boldsymbol{Z}_{22} + \alpha_z \boldsymbol{Z}_{23}\right) \\ & + \delta\phi_z \left(\alpha_x \boldsymbol{Z}_{31} + \alpha_y \boldsymbol{Z}_{32} + \alpha_z \boldsymbol{Z}_{33}\right) \end{aligned} \quad (.16)$$

in which:

$$\boldsymbol{Z}_{r,d} = \boldsymbol{U}^T \bar{\boldsymbol{A}}_r^T \boldsymbol{M}\bar{\boldsymbol{A}}_d \boldsymbol{U} \quad (.17)$$

for $r = 1, 2, 3$ and $d = 1, 2, 3$. At the same time:

$$\begin{aligned} \boldsymbol{U}^T \delta\bar{\boldsymbol{\Phi}}^T \boldsymbol{M}\bar{\boldsymbol{\Omega}}\boldsymbol{U} = {} & \delta\phi_x \left(\omega_x \boldsymbol{Z}_{11} + \omega_y \boldsymbol{Z}_{12} + \omega_z \boldsymbol{Z}_{13}\right) \\ & + \delta\phi_y \left(\omega_x \boldsymbol{Z}_{21} + \omega_y \boldsymbol{Z}_{22} + \omega_z \boldsymbol{Z}_{23}\right) \\ & + \delta\phi_z \left(\omega_x \boldsymbol{Z}_{31} + \omega_y \boldsymbol{Z}_{32} + \omega_z \boldsymbol{Z}_{33}\right) \end{aligned} \quad (.18)$$

The term:

$$\begin{aligned} \boldsymbol{U}^T \delta\boldsymbol{U}^T \delta\bar{\boldsymbol{\Phi}}^T \boldsymbol{M}\bar{\boldsymbol{\Omega}}^T \bar{\boldsymbol{\Omega}}\boldsymbol{U} = {} & \boldsymbol{U}^T \left(\delta\phi_x \bar{\boldsymbol{A}}_1^T + \delta\phi_y \bar{\boldsymbol{A}}_2^T + \delta\phi_z \bar{\boldsymbol{A}}_3^T\right) \boldsymbol{M} \\ & \left((\omega_y^2 + \omega_z^2)\bar{\boldsymbol{S}}_1 + (\omega_x^2 + \omega_z^2)\bar{\boldsymbol{S}}_2 + (\omega_x^2 + \omega_y^2)\bar{\boldsymbol{S}}_3 + \omega_x\omega_y\bar{\boldsymbol{S}}_4 + \omega_x\omega_z\bar{\boldsymbol{S}}_5 + \omega_y\omega_z\bar{\boldsymbol{S}}_6\right) \boldsymbol{U} \end{aligned} \quad (.19)$$

can be written as:

$$\begin{aligned} & \boldsymbol{U}^T \delta\bar{\boldsymbol{\Phi}}^T \boldsymbol{M}\bar{\boldsymbol{\Omega}}^T \bar{\boldsymbol{\Omega}}\boldsymbol{U} = \\ & \delta\phi_x \left((\omega_y^2 + \omega_z^2)\boldsymbol{W}_{11} + (\omega_x^2 + \omega_z^2)\boldsymbol{W}_{12} + (\omega_x^2 + \omega_y^2)\boldsymbol{W}_{13} + \omega_x\omega_y\boldsymbol{W}_{14} + \omega_x\omega_z\boldsymbol{W}_{15} + \omega_y\omega_z\boldsymbol{W}_{16}\right) \\ & + \delta\phi_y \left((\omega_y^2 + \omega_z^2)\boldsymbol{W}_{21} + (\omega_x^2 + \omega_z^2)\boldsymbol{W}_{22} + (\omega_x^2 + \omega_y^2)\boldsymbol{W}_{23} + \omega_x\omega_y\boldsymbol{W}_{24} + \omega_x\omega_z\boldsymbol{W}_{25} + \omega_y\omega_z\boldsymbol{W}_{26}\right) \\ & + \delta\phi_z \left((\omega_y^2 + \omega_z^2)\boldsymbol{W}_{31} + (\omega_x^2 + \omega_z^2)\boldsymbol{W}_{32} + (\omega_x^2 + \omega_y^2)\boldsymbol{W}_{33} + \omega_x\omega_y\boldsymbol{W}_{34} + \omega_x\omega_z\boldsymbol{W}_{35} + \omega_y\omega_z\boldsymbol{W}_{36}\right) \end{aligned} \quad (.20)$$

where:

$$\boldsymbol{W}_{r,t} = \boldsymbol{U}^T \bar{\boldsymbol{A}}_r^T \boldsymbol{M}\bar{\boldsymbol{S}}_t \boldsymbol{U} \quad (.21)$$

for $r = 1, 2, 3$ and $t = 1, 2, 3, 4, 5, 6$.

APPENDIX D: Development of terms $\hat{\boldsymbol{i}}$

If the nodes do not have rotational DoFs, only gravity forces (not torques) are applied to them. In this case:

$$\begin{aligned}
\hat{\boldsymbol{i}}_1 &= \begin{bmatrix} 1 & 0 & 0 & 1 & 0 & 0 & 1 & 0 & 0 & 1 & 0 & 0 & \dots \end{bmatrix}^T \\
\hat{\boldsymbol{i}}_2 &= \begin{bmatrix} 0 & 1 & 0 & 0 & 1 & 0 & 0 & 1 & 0 & 0 & 1 & 0 & \dots \end{bmatrix}^T \\
\hat{\boldsymbol{i}}_3 &= \begin{bmatrix} 0 & 0 & 1 & 0 & 0 & 1 & 0 & 0 & 1 & 0 & 0 & 1 & \dots \end{bmatrix}^T
\end{aligned} \tag{.22}$$

It is worth to introduce the notation:

$$\hat{\boldsymbol{I}} = \begin{bmatrix} \boldsymbol{I} & \boldsymbol{I} & \boldsymbol{I} & \boldsymbol{I} & \dots & \boldsymbol{I} \end{bmatrix}^T \tag{.23}$$

where $\mathbf{I}$ are 3×3 identity matrices. Conversely, if nodes have rotational DoFs, $\hat{\boldsymbol{i}}_i$ are defined as:

$$\begin{aligned}
\hat{\boldsymbol{i}}_1 &= \begin{bmatrix} 1 & 0 & 0 & 0 & 0 & 0 & 1 & 0 & 0 & 0 & 0 & 0 & \dots \end{bmatrix}^T \\
\hat{\boldsymbol{i}}_2 &= \begin{bmatrix} 0 & 1 & 0 & 0 & 0 & 0 & 0 & 1 & 0 & 0 & 0 & 0 & \dots \end{bmatrix}^T \\
\hat{\boldsymbol{i}}_3 &= \begin{bmatrix} 0 & 0 & 1 & 0 & 0 & 0 & 0 & 0 & 1 & 0 & 0 & 0 & \dots \end{bmatrix}^T
\end{aligned} \tag{.24}$$

and the matrix $\hat{\boldsymbol{I}}$, is in this case:

$$\hat{\boldsymbol{I}} = \begin{bmatrix} \boldsymbol{I} & \mathbf{0} & \boldsymbol{I} & \mathbf{0} & \dots & \mathbf{0} \end{bmatrix}^T \tag{.25}$$

where $\mathbf{I}$ and $\mathbf{0}$ are 3×3 unit and zero matrices. Note that matrix $\mathbf{I}$ has been defined for the case where all the nodes have rotational DoFs or for the opposite case, where none of them has rotational DoFs. In case where nodes with rotational DoFs and nodes without are present in the same link, the development of the definition of $\mathbf{I}$ is straightforward.

References

ANSYS (2011), `http://www.ansys.com`.

Bauchau OA (2011), *Flexible Multibody Dynamics*, Springer.

Ben-Israel A and Greville TN (2003), *Generalized inverses. Theory and applications (2nd ed.)*, NY: Springer.

Benosman M, Boyer F, Vey G and Primautt D (2002), Flexible links manipulators: from modelling to control, *Journal of Intelligent and Robotic Systems* 34(4): 381–414.

Besselink B, Tabak U, Lutowska A, Wouw NVD, Nijmeijer H, Rixen D, Hochstenbach M and Schilders W (2013), A comparison of model reduction techniques from structural dynamics, numerical mathematics and systems and control, *Journal of Sound and Vibration* 332(19): 4403–4422.

Boscariol P and Zanotto V (2012), Design of a controller for trajectory tracking for compliant mechanisms with effective vibration suppression, *Robotica* 30: 15–29.

Boschetti G, Richiedei D and Trevisani A (2012), Delayed reference control applied to flexible link mechanisms: A scheme for effective and stable control, *Journal of Dynamic Systems, Measurement and Control* 134(1): 011003.

Caracciolo R, Richiedei D, Trevisani A and Zanotto V (2005), Robust mixed-norm position and vibration control of flexible link mechanisms, *Mechatronics* 15(7): 767–791.

Chang L and Hamilton J (1991), The kinematics of robotic manipulators with flexible links using an equivalent rigid link system (ERLS) model, *ASME Journal of Dynamic Systems, Measurement and Control* 113: 48–53.

Choi S and Cheon J (2004), Vibration control of a single-link flexible arm subjected to disturbances, *Journal of Sound and Vibration* 271: 1147–1156.

Craig R and Bampton M (1968), Coupling of substructures for dynamics analyses, *AIAA Journal* 6(7): 1313–1319.

Denavit J and Hartenberg R (1955), A kinematic notation for lower-pair mechanisms based on matrices, *ASME Journal of Applied Mechanics* 23: 215–221.

Dietz S, Wallrapp O and Wiedemann S (2003), Nodal vs. Modal representation in flexible multibody system dynamics, in: *Proceeding of MULTIBODY DYNAMICS 2003, IDMEC/IST 2003*, Lisbon, Portugal.

Dwivedy S and Eberhard P (2006), Dynamic analysis of flexible manipulators, a literature review, *Mechanism and Machine Theory* 41: 749–777.

Garca-Vallejo D, Mayo J, Escalona J and Dominguez J (2008), Three-dimensional formulation of rigid-flexible multibody systems with flexible beam elements, *Multibody Systems Dynamics* 20: 1–28.

Gasparetto A (2001), Accurate Modelling of a Flexible-Link Planar Mechanism by Means of a Linearized Model in the State-Space Form for Design of a Vibration Controller, *Journal of Sound and Vibration* 240(2): 241–262.

Gasparetto A, Giovagnoni M and Moosavi A (2013), Experimental Validation of a dynamic model for lightweight robots, *International Journal of Advanced Robotic Systems Industrial Robots* .

Gasparetto A and Zanotto V (2006), Vibration reduction in a flexible-link mechanism through synthesis of an optimal controller, *Meccanica* 6(6): 611–622.

Ge S, Lee T and Zhu G (1997), Nonlinear feedback controller for a single-link flexible manipulator based on finite element model, *J. Robotic Systems* 14(3): 165–178.

Giovagnoni M (1994), A Numerical and Experimental Analysis of a Chain of Flexible Bodies, *ASME Journal of Dynamic Systems, Measurement and Control* 116: 73–80.

Kalra P and Sharan A (1991), Accurate modeling of flexible manipulators using finite element analysis, *Mechanism and Machine Theory* 26: 299–313.

Koutsovasilis P and Beitelschmidt M (2008), Comparison of model reduction techniques for large mechanical systems : AA study on an elastic rod, *Multibody System Dynamics* 20(2): 111–128.

Martins J, Mohamed Z, Tokhi M, da Costa JS and Botto M (2003), Approaches for dynamic modelling of flexible manipulator systems, in: *Proceedings of the* IEEE Conference on Control Theory Appl., volume 150.

Naganathan G and Soni A (1988), Nonlinear modeling of kinematic and flexibility effects in manipulator design, *ASME Journal of Mechanisms, Transmission and Automation in Design* 110: 243–254.

Nagarajan S and Turcic D (1990), Lagrangian formulation of the equations of motion for elastic mechanisms with mutual dependence between rigid body and elastic motions. Part I: element level equations, *ASME Journal of Dynamic Systems, Measurements, and Control* 112: 203–214.

Ouyang H, Richiedei D and Trevisani A (2013), Pole assignment for control of flexible link mechanisms, *Journal of Sound and Vibration* 332(12): 2884–2899.

Palomba I, Richiedei D and Trevisani A (2014), A ranking method for the selection of the interior modes of reduced order resonant system models, in: *Proceeding of ASME 2014 12th Biennial Conference on Engineering Systems Design and Analysis, ESDA 2014*, volume 2.

Qu ZQ (2004), *Model Order Reduction Techniques with Applications in Finite Element Analysis*, Springer.

Shabana A (1997), Flexible Multibody Dynamics: Review of Past and Recent Developments, *Multibody System Dynamics* 1: 189–222.

Shabana A (2005), *Dynamics of Multibody systems, 3rd ed*, Cambridge University press.

Theodore R and Ghosal A (1995), Comparison of the assumed modes method and finite element models for flexible multilink manipulators, *Int. J. Robotics Res.* 14(2): 91–111.

Tokhi M and Azad A (2008), *Flexible Robot Manipulators: Modeling, Simulation and Control*, Control Engineering Series, The Institution of Engineering and Technology (IET).

Trevisani A (2003), Feedback control of flexible four-bar linkages: a numerical and experimental investigation, *Journal of Sound and Vibration* 268(5): 947–970.

Turcic D and Midha A (1984a), Dynamic analysis of elastic mechanism systems. part I: applications, *ASME Journal of Dynamic Systems, Measurement and Control* 106: 249–254.

Turcic D and Midha A (1984b), Generalized equations of motion for the dynamic analysis of elastic mechanism systems, *ASME Journal of Dynamic Systems, Measurement and Control* 106: 242–248.

Turcic D, Midha A and Bosnik J (1984), Dynamic analysis of elastic mechanism systems. part II: experiment results, *ASME Journal of Dynamic Systems, Measurement and Control* 106: 255–260.

Vidoni R, Gasparetto A and Giovagnoni M (2013), Design and implementation of an ERLS-based 3-D dynamic formulation for flexible-link robots, *Robotics and Computer-Integrated Manufacturing* 29: 273–282.

Vidoni R, Gasparetto A and Giovagnoni M (2014), A method for modeling three-dimensional flexible mechanisms based on an equivalent rigid link system, *Journal of Vibration and Control* 20(4): 483–500.

Wang D, Lu Y, Liu Y and Li X (1996), Dynamic model and tip trajectory tracking control for a two-link flexible robotic manipulator, in: *Proceedings of the* IEEE Conference on System, Man and Cybernetics, Beijing, pp. 1020–1024.

Wasfy TM and Noor AK (2003), Computational strategies for flexible multibody systems, *ASME Applied Mechanics Reviews* 56(6).